

Gutzwiller Density Functional Theory: a formal derivation and application to ferromagnetic nickel

Tobias Schickling¹, Jörg Bünemann¹, Florian Gebhard^{1,2}, and
Werner Weber^{3,†}

¹ Fachbereich Physik, Philipps Universität Marburg, D-35032 Marburg, Germany

² Material Sciences Center, Philipps Universität Marburg, D-35032 Marburg,
Germany

³ Institut für Physik, Technische Universität Dortmund, D-44227 Dortmund,
Germany

Abstract. We present a detailed derivation of the Gutzwiller Density Functional Theory that covers all conceivable cases of symmetries and Gutzwiller wave functions. The method is used in a study of ferromagnetic nickel where we calculate ground state properties (lattice constant, bulk modulus, spin magnetic moment) and the quasi-particle band structure. Our method resolves most shortcomings of an ordinary Density Functional calculation on nickel. However, the quality of the results strongly depends on the particular choice of the double-counting correction. This constitutes a serious problem for all methods that attempt to merge Density Functional Theory with correlated-electron approaches based on Hubbard-type local interactions.

To be published in *New Journal of Physics*, September 2014

† deceased on July 3, 2014

1. Introduction

Density Functional Theory (DFT) is the workhorse of electronic structure theory [1]. Based on the Hohenberg-Kohn theorem [1], the ground-state properties of an interacting many-electron system are calculated from those of an effective single-particle problem that can be solved numerically. An essential ingredient in DFT is the so-called exchange-correlation potential which, however, is unknown and sensible approximations must be devised, e.g., the local (spin) density approximation, L(S)DA. In this way, the electronic properties of metals were calculated systematically [2]. Unfortunately, the L(S)DA leads to unsatisfactory results for transition metals, their compounds, and for heavy-fermion systems. The electrons in the narrow $3d$ or $4f/5f$ bands experience correlations that are not covered by current exchange-correlation potentials.

For a more accurate description of electronic correlations in narrow bands, Hubbard-type models [3, 4] have been put forward. However, simplistic model Hamiltonians can describe limited aspects of real materials at best, while, at the same time, they reintroduce the full complexity of the many-body problem. Recently, new methods were developed that permit the (numerical) analysis of multi-band Hubbard models, and, moreover, can be combined with DFT, specifically, the LDA+ U method [5], the LDA+DMFT (Dynamical Mean-Field Theory) [6, 7], and the Gutzwiller variational approach [8, 9, 10, 11]. The LDA+ U approach treats atomic interactions on a mean-field level so that it is computationally cheap but it ignores true many-body correlations. The DMFT becomes formally exact for infinite lattice coordination number, $Z \rightarrow \infty$, but it requires the self-consistent solution of a dynamical impurity problem that is numerically very demanding. The Gutzwiller DFT is based on a variational treatment of local many-body correlations. Expectation values can be calculated for $Z \rightarrow \infty$ without further approximations, and the remaining computational problem remains tractable.

Previously, we used the DFT to obtain the bare band structure from which we calculated the properties of nickel [8, 12, 13, 14] and LaOFeAs [15]. For these studies, we developed a formalism that applies to general Gutzwiller-correlated states for arbitrary multi-band Hubbard Hamiltonians. However, some single-particle properties remained fixed at their DFT values. In contrast, in Refs. [9, 10, 11] the correlated electron density was fed back into the DFT calculations but the Gutzwiller quasi-particle Hamiltonian was introduced in an ad-hoc manner. In this work, we present a formal derivation of the Gutzwiller DFT as a generic extension of the DFT. Our formulae apply for general Gutzwiller-correlated wave functions and reproduce expressions used previously [9, 10] as special cases; for a recent application to topological insulators, see Ref. [16]. Here, we give results for nickel in face-centered cubic structure. The Gutzwiller DFT results for the lattice constant, the magnetic spin-only moment, and the bulk modulus agree very well with experiments. Moreover, the quasi-particle bandstructure from Gutzwiller DFT is in satisfactory agreement with data from Angle-Resolved Photo-Emission Spectroscopy (ARPES). As found earlier [9, 10], the Gutzwiller DFT overcomes the limitations of DFT for the description of transition metals.

Our paper is organized as follows. In Sect. 2 we recall the derivation of Density Functional Theory (DFT) as a variational approach to the many-body problem and its mapping to an effective single-particle reference system (Kohn-Sham scheme). We extend our concise derivation to many-particle reference systems in Sect. 3. In particular, we formulate the Gutzwiller density functional whose minimization leads to the Gutzwiller–Kohn-Sham Hamiltonian. The theory is worked out in the limit of large coordination number, $Z \rightarrow \infty$, where explicit expressions for the Gutzwiller density functional are available. In Sect. 4 we restrict ourselves to lattice systems that are invariant under translation by a lattice vector so that the quasi-particle excitations can be characterized by their Bloch momentum. In Sect. 5 we present results for face-centered cubic (fcc) nickel where $Z = 12$. A short summary, Sect. 6, closes our presentation. Technical details are deferred to the appendices.

2. Density Functional Theory

We start our presentation with a concise derivation of Density Functional Theory that can readily be extended to the Gutzwiller Density Functional Theory.

2.1. Many-particle Hamiltonian and Ritz variational principle

Our many-particle Hamiltonian for electrons with spin $\sigma = \uparrow, \downarrow$ reads ($\hbar \equiv 1$)

$$\begin{aligned}\hat{H} &= \hat{H}_{\text{band}} + \hat{H}_{\text{int}} , \\ \hat{H}_{\text{band}} &= \sum_{\sigma} \int d\mathbf{r} \hat{\Psi}_{\sigma}^{\dagger}(\mathbf{r}) \left(-\frac{\Delta_{\mathbf{r}}}{2m} + U(\mathbf{r}) \right) \hat{\Psi}_{\sigma}(\mathbf{r}) , \\ \hat{H}_{\text{int}} &= \sum_{\sigma, \sigma'} \int d\mathbf{r} \int d\mathbf{r}' \hat{\Psi}_{\sigma}^{\dagger}(\mathbf{r}) \hat{\Psi}_{\sigma'}^{\dagger}(\mathbf{r}') V(\mathbf{r} - \mathbf{r}') \hat{\Psi}_{\sigma'}(\mathbf{r}') \hat{\Psi}_{\sigma}(\mathbf{r})\end{aligned}\tag{1}$$

with

$$V(\mathbf{r} - \mathbf{r}') = \frac{1}{2} \frac{e^2}{|\mathbf{r} - \mathbf{r}'|} .\tag{2}$$

The electrons experience the periodic potential of the ions, $U(\mathbf{r})$, and their mutual Coulomb interaction, $V(\mathbf{r} - \mathbf{r}')$. The total number of electrons is $N = N_{\uparrow} + N_{\downarrow}$. According to the Ritz variational principle, the ground state of a Hamiltonian \hat{H} can be obtained from the minimization of the energy functional

$$E[\{|\Psi\rangle\}] = \langle \Psi | \hat{H} | \Psi \rangle\tag{3}$$

in the subset of normalized states $|\Psi\rangle$ in the Hilbert space with N electrons, $\langle \Psi | \Psi \rangle = 1$.

2.2. Levy's constrained search

The minimization of the energy functional (3) is done in two steps, the constrained search [17], Sect. 2.2.1, and the minimization of the density functional, Sect. 2.2.2.

To this end, we consider the subset of normalized states $|\Psi^{(n)}\rangle$ with fixed electron densities $n_\sigma(\mathbf{r})$,

$$n_\sigma(\mathbf{r}) = \langle \Psi^{(n)} | \hat{\Psi}_\sigma^\dagger(\mathbf{r}) \hat{\Psi}_\sigma(\mathbf{r}) | \Psi^{(n)} \rangle . \quad (4)$$

In the following we accept ‘physical’ densities only, i.e., those $n_\sigma(\mathbf{r})$ for which states $|\Psi^{(n)}\rangle$ can be found. For the subset of states $|\Psi^{(n)}\rangle$ we define

$$\hat{H}_e = \hat{H}_{\text{kin}} + \hat{V}_{\text{xc}} , \quad (5)$$

$$\hat{H}_{\text{kin}} = \sum_\sigma \int d\mathbf{r} \hat{\Psi}_\sigma^\dagger(\mathbf{r}) \left(-\frac{\Delta_{\mathbf{r}}}{2m} \right) \hat{\Psi}_\sigma(\mathbf{r}) , \quad (6)$$

$$\begin{aligned} \hat{V}_{\text{xc}} = \sum_{\sigma, \sigma'} \int d\mathbf{r} \int d\mathbf{r}' V(\mathbf{r} - \mathbf{r}') & \left[\hat{\Psi}_\sigma^\dagger(\mathbf{r}) \hat{\Psi}_{\sigma'}^\dagger(\mathbf{r}') \hat{\Psi}_{\sigma'}(\mathbf{r}') \hat{\Psi}_\sigma(\mathbf{r}) \right. \\ & \left. - \hat{\Psi}_\sigma^\dagger(\mathbf{r}) \hat{\Psi}_\sigma(\mathbf{r}) n_{\sigma'}(\mathbf{r}') - \hat{\Psi}_{\sigma'}^\dagger(\mathbf{r}') \hat{\Psi}_{\sigma'}(\mathbf{r}') n_\sigma(\mathbf{r}) + n_\sigma(\mathbf{r}) n_{\sigma'}(\mathbf{r}') \right] . \end{aligned} \quad (7)$$

Here, we extracted the Hartree terms from the Coulomb interaction H_{int} in eq. (1) so that \hat{V}_{xc} contains only the so-called exchange and correlation contributions. In the subset of normalized states $|\Psi^{(n)}\rangle$ we consider the functional

$$F \left[\{n_\sigma(\mathbf{r})\} , \{|\Psi^{(n)}\rangle\} \right] = \langle \Psi^{(n)} | \hat{H}_e | \Psi^{(n)} \rangle . \quad (8)$$

For fixed densities $n_\sigma(\mathbf{r})$, the Hamiltonian \hat{H}_e defines an electronic problem where the periodic potential of the ions is formally absent.

2.2.1. Constrained search. The formal task is to find the minimum of the energy functional F in (8) with respect to $|\Psi^{(n)}\rangle$,

$$\bar{F} [\{n_\sigma(\mathbf{r})\}] = \text{Min}_{\{|\Psi^{(n)}\rangle\}} F [\{n_\sigma(\mathbf{r})\} , \{|\Psi^{(n)}\rangle\}] . \quad (9)$$

Recall that the electron densities $n_\sigma(\mathbf{r})$ are fixed in this step. We denote the resulting optimal many-particle state $|\Psi_0^{(n)}\rangle$. Thus, we may write

$$\bar{F} [\{n_\sigma(\mathbf{r})\}] = F [\{n_\sigma(\mathbf{r})\} , \{|\Psi_0^{(n)}\rangle\}] = \langle \Psi_0^{(n)} | \hat{H}_e | \Psi_0^{(n)} \rangle . \quad (10)$$

For later use, we define the functionals for the kinetic energy

$$K [\{n_\sigma(\mathbf{r})\}] = \langle \Psi_0^{(n)} | \hat{H}_{\text{kin}} | \Psi_0^{(n)} \rangle \quad (11)$$

and the exchange-correlation energy

$$E_{\text{xc}} [\{n_\sigma(\mathbf{r})\}] = \langle \Psi_0^{(n)} | \hat{V}_{\text{xc}} | \Psi_0^{(n)} \rangle \quad (12)$$

so that

$$\bar{F} [\{n_\sigma(\mathbf{r})\}] = K [\{n_\sigma(\mathbf{r})\}] + E_{\text{xc}} [\{n_\sigma(\mathbf{r})\}] . \quad (13)$$

2.2.2. *Density functional, ground-state density and ground-state energy.* After the constrained search as a first step, we are left with the density functional

$$\begin{aligned} D[\{n_\sigma(\mathbf{r})\}] &= \bar{F}[\{n_\sigma(\mathbf{r})\}] + U[\{n_\sigma(\mathbf{r})\}] + V_{\text{Har}}[\{n_\sigma(\mathbf{r})\}] \\ &= K[\{n_\sigma(\mathbf{r})\}] + U[\{n_\sigma(\mathbf{r})\}] + V_{\text{Har}}[\{n_\sigma(\mathbf{r})\}] + E_{\text{xc}}[\{n_\sigma(\mathbf{r})\}] \end{aligned} \quad (14)$$

with

$$\begin{aligned} U[\{n_\sigma(\mathbf{r})\}] &= \sum_\sigma \int d\mathbf{r} U(\mathbf{r}) n_\sigma(\mathbf{r}) , \\ V_{\text{Har}}[\{n_\sigma(\mathbf{r})\}] &= \sum_{\sigma, \sigma'} \int d\mathbf{r} \int d\mathbf{r}' V(\mathbf{r} - \mathbf{r}') n_\sigma(\mathbf{r}) n_{\sigma'}(\mathbf{r}') . \end{aligned} \quad (15)$$

According to the Ritz variational principle, the ground-state energy E_0 is found from the minimization of this functional over the densities $n_\sigma(\mathbf{r})$,

$$E_0 = \text{Min}_{\{n_\sigma(\mathbf{r})\}} D[\{n_\sigma(\mathbf{r})\}] . \quad (16)$$

The ground-state densities $n_\sigma^0(\mathbf{r})$ are those where the minimum of $D[\{n_\sigma(\mathbf{r})\}]$ is obtained.

2.3. Single-particle reference system

We consider the subset of single-particle product states $|\Phi^{(n)}\rangle$ that are normalized to unity, $\langle \Phi^{(n)} | \Phi^{(n)} \rangle = 1$. As before, the upper index indicates that they all lead to the same (physical) single-particle densities $n_\sigma^{\text{sp}}(\mathbf{r})$,

$$n_\sigma^{\text{sp}}(\mathbf{r}) = \langle \Phi^{(n)} | \hat{\Psi}_\sigma^\dagger(\mathbf{r}) \hat{\Psi}_\sigma(\mathbf{r}) | \Phi^{(n)} \rangle . \quad (17)$$

As our single-particle Hamiltonian we consider the kinetic-energy operator \hat{H}_{kin} , see eq. (6). For fixed single-particle densities $n_\sigma^{\text{sp}}(\mathbf{r})$ we define the single-particle kinetic-energy functional

$$F_{\text{sp}}[\{n_\sigma^{\text{sp}}(\mathbf{r})\}, \{|\Phi^{(n)}\rangle\}] = \langle \Phi^{(n)} | \hat{H}_{\text{kin}} | \Phi^{(n)} \rangle . \quad (18)$$

2.3.1. *Constrained search.* As in Sect. 2.2, we carry out a constrained search in the subset of states $|\Phi^{(n)}\rangle$. The task is the minimization of the kinetic-energy functional $F_{\text{sp}}[\{n_\sigma^{\text{sp}}(\mathbf{r})\}, \{|\Phi^{(n)}\rangle\}]$. We denote the optimized single-particle product state $|\Phi_0^{(n)}\rangle$ so that we find the density functional for the kinetic energy as

$$\bar{F}_{\text{sp}}[\{n_\sigma^{\text{sp}}(\mathbf{r})\}] = \langle \Phi_0^{(n)} | \hat{H}_{\text{kin}} | \Phi_0^{(n)} \rangle \equiv K_{\text{sp}}[\{n_\sigma^{\text{sp}}(\mathbf{r})\}] . \quad (19)$$

2.3.2. *Single-particle density functional.* As the density functional $D_{\text{sp}}[\{n_\sigma^{\text{sp}}(\mathbf{r})\}]$ that corresponds to the single-particle problem we define

$$\begin{aligned} D_{\text{sp}}[\{n_\sigma^{\text{sp}}(\mathbf{r})\}] &= K_{\text{sp}}[\{n_\sigma^{\text{sp}}(\mathbf{r})\}] + U[\{n_\sigma^{\text{sp}}(\mathbf{r})\}] + V_{\text{Har}}[\{n_\sigma^{\text{sp}}(\mathbf{r})\}] \\ &\quad + E_{\text{sp,xc}}[\{n_\sigma^{\text{sp}}(\mathbf{r})\}] , \end{aligned} \quad (20)$$

with the kinetic energy term from (19), the contributions from the external potential and the Hartree terms $U[\{n_\sigma^{\text{sp}}(\mathbf{r})\}]$ and $V_{\text{Har}}[\{n_\sigma^{\text{sp}}(\mathbf{r})\}]$ from eq. (15), and the single-particle exchange-correlation potential $E_{\text{sp,xc}}[\{n_\sigma^{\text{sp}}(\mathbf{r})\}]$ that we will specify later. The functional (20) defines our single-particle reference system.

2.3.3. Noninteracting V -representability. In order to link the many-particle and single-particle approaches we make the assumption of non-interacting V -representability [1]: For any given (physical) densities $n_\sigma(\mathbf{r})$ we can find a subset of normalized single-particle product states $|\Phi^{(n)}\rangle$ with N electrons such that

$$n_\sigma^{\text{sp}}(\mathbf{r}) = n_\sigma(\mathbf{r}) . \quad (21)$$

Moreover, we demand that the density functionals $D[\{n_\sigma(\mathbf{r})\}]$ (14) for the interacting electrons and $D_{\text{sp}}[\{n_\sigma(\mathbf{r})\}]$ (20) for the single-particle problem agree with each other [18],

$$D_{\text{sp}}[\{n_\sigma(\mathbf{r})\}] = D[\{n_\sigma(\mathbf{r})\}] . \quad (22)$$

Then, the single-particle problem leads to the same ground-state density $n_\sigma^0(\mathbf{r})$ and ground-state energy E_0 as the interacting-particle Hamiltonian because the density variation is done with the same density functional (Hohenberg-Kohn theorem) [1].

The condition (22) is equivalent to

$$K_{\text{sp}}[\{n_\sigma(\mathbf{r})\}] + E_{\text{sp,xc}}[\{n_\sigma(\mathbf{r})\}] = K[\{n_\sigma(\mathbf{r})\}] + E_{\text{xc}}[\{n_\sigma(\mathbf{r})\}] \quad (23)$$

because the interaction with the external potential and the Hartree term only depend on the densities. Eq. (23) then leads to an exact expression for the single-particle exchange-correlation energy

$$E_{\text{sp,xc}}[\{n_\sigma(\mathbf{r})\}] = K[\{n_\sigma(\mathbf{r})\}] - K_{\text{sp}}[\{n_\sigma(\mathbf{r})\}] + E_{\text{xc}}[\{n_\sigma(\mathbf{r})\}] . \quad (24)$$

This is our defining equation for $E_{\text{sp,xc}}[\{n_\sigma(\mathbf{r})\}]$ in eq. (20).

2.4. Kohn-Sham Hamiltonian

In the following we address the single-particle energy functional directly, i.e., the Ritz variational problem without a prior constrained search,

$$E[\{n_\sigma(\mathbf{r})\}, \{|\Phi\rangle\}] = \langle \Phi | \hat{H}_{\text{kin}} | \Phi \rangle + U[\{n_\sigma(\mathbf{r})\}] + V_{\text{Har}}[\{n_\sigma(\mathbf{r})\}] + E_{\text{sp,xc}}[\{n_\sigma(\mathbf{r})\}] . \quad (25)$$

For the extension to the Gutzwiller Density Functional Theory in Sect. 3, we expand the field operators in a basis,

$$\hat{\Psi}_\sigma(\mathbf{r}) = \sum_i \langle \mathbf{r} | i, \sigma \rangle \hat{c}_{i,\sigma} , \quad \hat{\Psi}_\sigma^\dagger(\mathbf{r}) = \sum_i \hat{c}_{i,\sigma}^\dagger \langle i, \sigma | \mathbf{r} \rangle , \quad (26)$$

where the index i represents a combination of site (or crystal momentum) index and an orbital index. For a canonical basis we must have completeness and orthogonality,

$$\sum_{i,\sigma} |i, \sigma\rangle \langle i, \sigma| = \hat{1} \quad , \quad \langle i, \sigma | j, \sigma' \rangle = \delta_{i,j} \delta_{\sigma,\sigma'} . \quad (27)$$

When we insert (26) into (6), we obtain the operator for the kinetic energy in a general single-particle basis,

$$\hat{H}_{\text{kin}} = \sum_{i,j,\sigma} T_{i,j;\sigma} \hat{c}_{i,\sigma}^\dagger \hat{c}_{j,\sigma} , \quad (28)$$

where the elements of the kinetic-energy matrix \tilde{T}_σ are given by

$$T_{i,j;\sigma} = \int d\mathbf{r} \xi_{i,\sigma}^*(\mathbf{r}) \left(-\frac{\Delta \mathbf{r}}{2m} \right) \xi_{j,\sigma}(\mathbf{r}) , \quad (29)$$

with $\xi_{i,\sigma}(\mathbf{r}) = \langle \mathbf{r} | i, \sigma \rangle$.

2.4.1. Energy functional. We introduce the single-particle density matrix $\tilde{\rho}$. Its elements in the general single-particle basis read

$$\rho_{(i,\sigma),(j,\sigma)} = \langle \Phi | \hat{c}_{j,\sigma}^\dagger \hat{c}_{i,\sigma} | \Phi \rangle \equiv \rho_{i,j;\sigma} . \quad (30)$$

Then, the densities are given by

$$n_\sigma(\mathbf{r}) = \sum_{i,j} \xi_{i,\sigma}^*(\mathbf{r}) \xi_{j,\sigma}(\mathbf{r}) \rho_{j,i;\sigma} . \quad (31)$$

Using these definitions, we can write the energy functional in the form

$$\begin{aligned} E[\{n_\sigma(\mathbf{r})\}, \tilde{\rho}] &= \sum_{i,j} \sum_{\sigma} T_{i,j;\sigma} \rho_{j,i;\sigma} + U[\{n_\sigma(\mathbf{r})\}] + V_{\text{Har}}[\{n_\sigma(\mathbf{r})\}] \\ &\quad + E_{\text{sp,xc}}[\{n_\sigma(\mathbf{r})\}] . \end{aligned} \quad (32)$$

The fact that $|\Phi\rangle$ are normalized single-particle product states is encoded in the matrix relation

$$\tilde{\rho} \cdot \tilde{\rho} = \tilde{\rho} . \quad (33)$$

This is readily proven by using a unitary transformation between the operators $\hat{c}_{i,\sigma}$ and the single-particle operators $\hat{b}_{k,\sigma}$ that generate $|\Phi\rangle$, see Appendix A.1.

When we minimize $E[\{n_\sigma(\mathbf{r})\}, \tilde{\rho}]$ with respect to $\tilde{\rho}$ we must take the condition (33) into account using a matrix $\tilde{\Omega}$ of Lagrange multipliers $\Omega_{l,m;\sigma}$. Moreover, we use the Lagrange multipliers $\kappa_\sigma(\mathbf{r})$ to ensure eq. (31), i.e., altogether we address the functional $G_{\text{DFT}} \equiv G_{\text{DFT}}[\tilde{\rho}, \tilde{\Omega}, \{n_\sigma(\mathbf{r})\}, \{\kappa_\sigma(\mathbf{r})\}]$

$$\begin{aligned} G_{\text{DFT}} &= E[\{n_\sigma(\mathbf{r})\}, \tilde{\rho}] - \sum_{l,m,\sigma} \Omega_{l,m;\sigma} \left(\sum_p \rho_{l,p;\sigma} \rho_{p,m;\sigma} - \rho_{l,m;\sigma} \right) \\ &\quad - \sum_{\sigma} \int d\mathbf{r} \kappa_\sigma(\mathbf{r}) \left(n_\sigma(\mathbf{r}) - \sum_{i,j} \xi_{i,\sigma}^*(\mathbf{r}) \xi_{j,\sigma}(\mathbf{r}) \rho_{j,i;\sigma} \right) . \end{aligned} \quad (34)$$

2.4.2. Minimization. When we minimize G_{DFT} in eq. (34) with respect to $n_\sigma(\mathbf{r})$ we find

$$\kappa_\sigma(\mathbf{r}) = U(\mathbf{r}) + V_{\text{Har}}(\mathbf{r}) + v_{\text{sp,xc},\sigma}(\mathbf{r}) , \quad (35)$$

$$V_{\text{Har}}(\mathbf{r}) \equiv \sum_{\sigma'} \int d\mathbf{r}' 2V(\mathbf{r} - \mathbf{r}') n_{\sigma'}^0(\mathbf{r}') , \quad (36)$$

$$\begin{aligned} v_{\text{sp,xc},\sigma}(\mathbf{r}) &\equiv \left. \frac{\partial E_{\text{sp,xc}}[\{n_{\sigma'}(\mathbf{r}')\}]}{\partial n_\sigma(\mathbf{r})} \right|_{n_\sigma(\mathbf{r})=n_\sigma^0(\mathbf{r})} \\ &= \left. \frac{\partial [K[\{n_{\sigma'}(\mathbf{r}')\}] - K_{\text{sp}}[\{n_{\sigma'}(\mathbf{r}')\}] + E_{\text{xc}}[\{n_{\sigma'}(\mathbf{r}')\}]]}{\partial n_\sigma(\mathbf{r})} \right|_{n_\sigma(\mathbf{r})=n_\sigma^0(\mathbf{r})} , \end{aligned} \quad (37)$$

where $V_{\text{Har}}(\mathbf{r})$ is the Hartree interaction and $v_{\text{sp,xc},\sigma}(\mathbf{r})$ is the single-particle exchange-correlation potential.

The minimization with respect to $\tilde{\rho}$ is outlined in Appendix A.2 [19]. It leads to the Kohn-Sham single-particle Hamiltonian

$$\hat{H}^{\text{KS}} = \sum_{i,j,\sigma} T_{i,j;\sigma}^{\text{KS}} \hat{c}_{i,\sigma}^\dagger \hat{c}_{j,\sigma} , \quad (38)$$

where the elements of the Kohn-Sham Hamilton matrix $\tilde{T}_\sigma^{\text{KS}}$ are given by

$$T_{i,j;\sigma}^{\text{KS}} = \frac{\partial E[\{n_\sigma(\mathbf{r})\}, \tilde{\rho}]}{\partial \rho_{j,i;\sigma}} + \int d\mathbf{r} \kappa_\sigma(\mathbf{r}) \xi_{i,\sigma}^*(\mathbf{r}) \xi_{j,\sigma}(\mathbf{r}) . \quad (39)$$

Explicitly,

$$T_{i,j;\sigma}^{\text{KS}} = \int d\mathbf{r} \xi_{i,\sigma}^*(\mathbf{r}) h_\sigma^{\text{KS}}(\mathbf{r}) \xi_{j,\sigma}(\mathbf{r}) , \quad (40)$$

$$h_\sigma^{\text{KS}}(\mathbf{r}) \equiv -\frac{\Delta_{\mathbf{r}}}{2m} + V_\sigma^{\text{KS}}(\mathbf{r}) , \quad (41)$$

$$V_\sigma^{\text{KS}}(\mathbf{r}) \equiv \kappa_\sigma(\mathbf{r}) = U(\mathbf{r}) + V_{\text{Har}}(\mathbf{r}) + v_{\text{sp,xc},\sigma}(\mathbf{r}) . \quad (42)$$

Here, we defined the ‘Kohn-Sham potential’ $V_\sigma^{\text{KS}}(\mathbf{r})$ that, in our derivation, is identical to the Lagrange parameter $\kappa_\sigma(\mathbf{r})$.

The remaining task is to find the basis in which the Kohn-Sham matrix $\tilde{T}_\sigma^{\text{KS}}$ is diagonal, see Appendix A.3.

3. Density Functional Theory for many-particle reference systems

The Kohn-Sham potential (37) cannot be calculated exactly because the functionals in eq. (24) are not known. Therefore, assumptions must be made about the form of the single-particle exchange-correlation potential, e.g., the Local Density Approximation [1]. Unfortunately, such approximations are not satisfactory for, e.g., transition metals and their compounds, and more sophisticated many-electron approaches must be employed.

3.1. Hubbard Hamiltonian and Hubbard density functional

3.1.1. Multi-band Hubbard model. A better description of transition metals and their compounds can be achieved by supplementing the single-particle reference system resulting from \hat{H}_{kin} in Sect. 2.3 by a multi-band Hubbard interaction. Then, our multi-band reference system follows from

$$\hat{H}_{\text{H}} = \hat{H}_{\text{kin}} + \hat{V}_{\text{loc}} - \hat{V}_{\text{dc}} , \quad (43)$$

where \hat{V}_{loc} describes local interactions between electrons in Wannier orbitals on the same site \mathbf{R} . The local single-particle operator \hat{V}_{dc} accounts for the double counting of their interactions in the Hubbard term \hat{V}_{loc} and in the single-particle exchange-correlation energy $E_{\text{sp,xc}}$. We assume that \hat{V}_{loc} and \hat{V}_{dc} do not depend on the densities $n_\sigma(\mathbf{r})$ explicitly.

For the local interaction we set

$$\begin{aligned} \hat{V}_{\text{loc}} &= \sum_{\mathbf{R}} \hat{V}_{\text{loc}}(\mathbf{R}) , \\ \hat{V}_{\text{loc}}(\mathbf{R}) &= \frac{1}{2} \sum_{(c_1,\sigma_1),\dots,(c_4,\sigma_4)} U_{(c_3,\sigma_3),(c_4,\sigma_4)}^{(c_1,\sigma_1),(c_2,\sigma_2)} \hat{c}_{\mathbf{R},c_1,\sigma_1}^\dagger \hat{c}_{\mathbf{R},c_2,\sigma_2}^\dagger \hat{c}_{\mathbf{R},c_3,\sigma_3} \hat{c}_{\mathbf{R},c_4,\sigma_4} . \end{aligned} \quad (44)$$

Note that only electrons in the small subset of correlated orbitals (index c) experience the two-particle interaction \hat{V}_{loc} : When there are two electrons in the Wannier orbitals

$\phi_{\mathbf{R},c_3,\sigma_3}(\mathbf{r})$ and $\phi_{\mathbf{R},c_4,\sigma_4}(\mathbf{r})$ centered around the lattice site \mathbf{R} , they are scattered into the orbitals $\phi_{\mathbf{R},c_1,\sigma_1}(\mathbf{r})$ and $\phi_{\mathbf{R},c_2,\sigma_2}(\mathbf{r})$, centered around the same lattice site \mathbf{R} ; for the definition of basis states, see Appendix A.3. Typically, we consider $c = 3d$ for the transition metals and their compounds.

The interaction strengths are parameters of the theory. Later, we shall employ the spherical approximation so that U_{\dots} for d -electrons can be expressed in terms of three Racah parameters A , B , and C . Fixing C/B makes it possible to introduce an effective Hubbard parameter U and an effective Hund's-rule coupling J , see Sect. 5 and Appendix C. Due to screening, the effective Hubbard interaction U is smaller than its bare, atomic value. In general, U and J are chosen to obtain good agreement with experiment, see Sect. 5.

3.1.2. Hubbard density functional. According to Levy's constrained search, we must find the minimum of the functional

$$F_{\text{H}} [\{n_{\sigma}(\mathbf{r})\}, \{|\Psi^{(n)}\rangle\}] = \langle \Psi^{(n)} | \hat{H}_{\text{H}} | \Psi^{(n)} \rangle \quad (45)$$

in the subset of normalized states with given (physical) density $n_{\sigma}(\mathbf{r})$, see eq. (4). The minimum of $F_{\text{H}} [\{n_{\sigma}(\mathbf{r})\}, \{|\Psi^{(n)}\rangle\}]$ over the states $|\Psi^{(n)}\rangle$ is the ground state $|\Psi_{\text{H},0}^{(n)}\rangle$ of the Hamiltonian \hat{H}_{H} for fixed densities $n_{\sigma}(\mathbf{r})$. In analogy to Sect. 2.3, we define the Hubbard density functional

$$\begin{aligned} D_{\text{H}} [\{n_{\sigma}(\mathbf{r})\}] &= K_{\text{H}} [\{n_{\sigma}(\mathbf{r})\}] + U [\{n_{\sigma}(\mathbf{r})\}] + V_{\text{Har}} [\{n_{\sigma}(\mathbf{r})\}] \\ &\quad + V_{\text{loc}} [\{n_{\sigma}(\mathbf{r})\}] - V_{\text{dc}} [\{n_{\sigma}(\mathbf{r})\}] + E_{\text{H,xc}} [\{n_{\sigma}(\mathbf{r})\}] , \end{aligned} \quad (46)$$

where

$$\begin{aligned} K_{\text{H}} [\{n_{\sigma}(\mathbf{r})\}] &= \langle \Psi_{\text{H},0}^{(n)} | \hat{H}_{\text{kin}} | \Psi_{\text{H},0}^{(n)} \rangle , \\ V_{\text{loc/dc}} [\{n_{\sigma}(\mathbf{r})\}] &= \langle \Psi_{\text{H},0}^{(n)} | \hat{V}_{\text{loc/dc}} | \Psi_{\text{H},0}^{(n)} \rangle , \end{aligned} \quad (47)$$

and $E_{\text{H,xc}} [\{n_{\sigma}(\mathbf{r})\}]$ is the exchange-correlation energy for \hat{H}_{H} . As in Sect. 2.3, the Hubbard density functional agrees with the exact density functional if we choose

$$\begin{aligned} E_{\text{H,xc}} [\{n_{\sigma}(\mathbf{r})\}] &= K [\{n_{\sigma}(\mathbf{r})\}] - K_{\text{H}} [\{n_{\sigma}(\mathbf{r})\}] \\ &\quad + E_{\text{xc}} [\{n_{\sigma}(\mathbf{r})\}] - (V_{\text{loc}} [\{n_{\sigma}(\mathbf{r})\}] - V_{\text{dc}} [\{n_{\sigma}(\mathbf{r})\}]) . \end{aligned} \quad (48)$$

Then, the Hubbard approach provides the exact ground-state densities and ground-state energy of our full many-particle Hamiltonian (Hubbard–Hohenberg–Kohn theorem). Of course, our derivation relies on the assumption of Hubbard V -representability of the densities $n_{\sigma}(\mathbf{r})$.

3.1.3. Hubbard single-particle potential. When we directly apply the Ritz principle, we have to minimize the energy functional $E \equiv E [\{n_{\sigma}(\mathbf{r})\}, \{|\Psi\rangle\}]$

$$E = \langle \Psi | \hat{H}_{\text{H}} | \Psi \rangle + U [\{n_{\sigma}(\mathbf{r})\}] + V_{\text{Har}} [\{n_{\sigma}(\mathbf{r})\}] + E_{\text{H,xc}} [\{n_{\sigma}(\mathbf{r})\}] . \quad (49)$$

We include the constraints eq. (4) and the normalization condition using the Lagrange parameters $\kappa_\sigma(\mathbf{r})$ and E_0 in the functional $G_H \equiv G_H[\{|\Psi\rangle\}, \{n_\sigma(\mathbf{r})\}, \{\kappa_\sigma(\mathbf{r})\}, E_0]$

$$G_H = E[\{n_\sigma(\mathbf{r})\}, \{|\Psi\rangle\}] - E_0(\langle\Psi|\Psi\rangle - 1) - \sum_\sigma \int d\mathbf{r} \kappa_\sigma(\mathbf{r}) (n_\sigma(\mathbf{r}) - \langle\Psi|\hat{\Psi}_\sigma^\dagger(\mathbf{r})\hat{\Psi}_\sigma(\mathbf{r})|\Psi\rangle). \quad (50)$$

As in Sect. 2.4, see eqs. (35) and (42), the variation of G_H with respect to $n_\sigma(\mathbf{r})$ gives the single-particle potential

$$V_\sigma^H(\mathbf{r}) \equiv U(\mathbf{r}) + V_{\text{Har}}(\mathbf{r}) + v_{\text{H,xc},\sigma}(\mathbf{r}), \quad v_{\text{H,xc},\sigma}(\mathbf{r}) \equiv \left. \frac{\partial E_{\text{H,xc}}[\{n_{\sigma'}(\mathbf{r}')\}]}{\partial n_\sigma(\mathbf{r})} \right|_{n_\sigma(\mathbf{r})=n_\sigma^0(\mathbf{r})}. \quad (51)$$

The Hubbard-model approach is based on the idea that typical approximations for the exchange-correlation energy, e.g., the local-density approximation, are suitable for the Hubbard model,

$$E_{\text{H,xc}}[\{n_\sigma(\mathbf{r})\}] \approx E_{\text{LDA,xc}}[\{n_\sigma(\mathbf{r})\}]. \quad (52)$$

Indeed, as seen from eq. (48), in the Hubbard exchange-correlation energy $E_{\text{H,xc}}$ the exchange-correlation contributions in the exact E_{xc} are reduced by the Hubbard term $V_{\text{loc}}[\{n_\sigma(\mathbf{r})\}] - V_{\text{dc}}[\{n_\sigma(\mathbf{r})\}]$, reflecting a more elaborate treatment of local correlations.

The minimization of (49) with respect to $|\Psi\rangle$ constitutes an unsolvable many-particle problem. The ground state $|\Psi_0\rangle$ is the solution of the many-particle Schrödinger equation with energy E_0 ,

$$(\hat{H}_0 + \hat{V}_{\text{loc}} - \hat{V}_{\text{dc}})|\Psi_0\rangle = E_0|\Psi_0\rangle \quad (53)$$

with the single-particle Hamiltonian

$$\hat{H}_0 = \sum_\sigma \int d\mathbf{r} \hat{\Psi}_\sigma^\dagger(\mathbf{r}) \left(-\frac{\Delta_{\mathbf{r}}}{2m} + U(\mathbf{r}) + V_{\text{Har}}(\mathbf{r}) + v_{\text{H,xc},\sigma}(\mathbf{r}) \right) \hat{\Psi}_\sigma(\mathbf{r}). \quad (54)$$

The Schrödinger equation (53) can be used as starting point for further approximations, for example, the Dynamical Mean-Field Theory (DMFT). In the following we will address the functional in eq. (49) directly.

3.2. Gutzwiller density functional

In the widely used LDA+ U approach [5], the functional in eq. (49) is evaluated and (approximately) minimized by means of single-particle product wave functions. However, this approach treats correlations only on a mean-field level. In the more sophisticated Gutzwiller approach, we consider the functional in eq. (49) in the subset of Gutzwiller-correlated variational many-particle states.

3.2.1. Gutzwiller variational ground state. In order to formulate the Gutzwiller variational ground state [4, 8], we consider the local (atomic) states $|\Gamma\rangle_{\mathbf{R}}$ that are built from the correlated orbitals. The local Hamiltonians take the form

$$\hat{V}_{\text{loc/dc}}(\mathbf{R}) = \sum_{\Gamma,\Gamma'} E_{\Gamma,\Gamma'}^{\text{loc/dc}}(\mathbf{R}) |\Gamma\rangle_{\mathbf{R}} \langle\Gamma'| = \sum_{\Gamma,\Gamma'} E_{\Gamma,\Gamma'}^{\text{loc/dc}}(\mathbf{R}) \hat{m}_{\mathbf{R},\Gamma,\Gamma'}, \quad (55)$$

where $|\Gamma\rangle_{\mathbf{R}}$ contains $|\Gamma_{\mathbf{R}}|$ electrons. Here, we introduced

$$E_{\Gamma,\Gamma'}^{\text{loc/dc}}(\mathbf{R}) = {}_{\mathbf{R}}\langle\Gamma|\hat{V}_{\text{loc/dc}}(\mathbf{R})|\Gamma'\rangle_{\mathbf{R}} \quad (56)$$

and the local many-particle operators $\hat{m}_{\mathbf{R};\Gamma,\Gamma'} = |\Gamma\rangle_{\mathbf{R}}\langle\Gamma'|$.

The Gutzwiller correlator and the Gutzwiller variational states are defined as

$$\hat{P}_G = \prod_{\mathbf{R}} \sum_{\Gamma,\Gamma'} \lambda_{\Gamma,\Gamma'}(\mathbf{R}) \hat{m}_{\mathbf{R};\Gamma,\Gamma'} \quad , \quad |\Psi_G\rangle = \hat{P}_G |\Phi\rangle . \quad (57)$$

Here, $|\Phi\rangle$ is a single-particle product state, and $\lambda_{\Gamma,\Gamma'}(\mathbf{R})$ defines the matrix $\tilde{\lambda}(\mathbf{R})$ of, in general, complex variational parameters.

3.2.2. Gutzwiller functionals. We evaluate the energy functional (49) in the restricted subset of Gutzwiller variational states,

$$\begin{aligned} E[\{n_{\sigma}(\mathbf{r})\}, \{|\Psi_G\rangle\}] &= \sum_{\mathbf{R},b,\mathbf{R}',b',\sigma} T_{(\mathbf{R},b),(\mathbf{R}',b');\sigma} \rho_{(\mathbf{R}',b'),(\mathbf{R},b);\sigma}^G + V_{\text{loc}}^G - V_{\text{dc}}^G \\ &\quad + U[\{n_{\sigma}(\mathbf{r})\}] + V_{\text{Har}}[\{n_{\sigma}(\mathbf{r})\}] + E_{\text{H,xc}}[\{n_{\sigma}(\mathbf{r})\}] , \\ V_{\text{loc/dc}}^G &= \sum_{\mathbf{R}} \sum_{\Gamma,\Gamma'} E_{\Gamma,\Gamma'}^{\text{loc/dc}}(\mathbf{R}) m_{\mathbf{R};\Gamma,\Gamma'}^G . \end{aligned} \quad (58)$$

Note that we work with the orbital Wannier basis, see Appendix A.3,

$$T_{(\mathbf{R},b),(\mathbf{R}',b');\sigma} = \int d\mathbf{r} \phi_{\mathbf{R},b,\sigma}^*(\mathbf{r}) \left(-\frac{\Delta_{\mathbf{r}}}{2m} \right) \phi_{\mathbf{R}',b',\sigma}(\mathbf{r}) . \quad (59)$$

The elements of the Gutzwiller-correlated single-particle density matrix are

$$\rho_{(\mathbf{R}',b'),(\mathbf{R},b);\sigma}^G = \frac{\langle \Psi_G | \hat{c}_{\mathbf{R},b,\sigma}^{\dagger} \hat{c}_{\mathbf{R}',b',\sigma} | \Psi_G \rangle}{\langle \Psi_G | \Psi_G \rangle} = \frac{\langle \Phi | \hat{P}_G^{\dagger} \hat{c}_{\mathbf{R},b,\sigma}^{\dagger} \hat{c}_{\mathbf{R}',b',\sigma} \hat{P}_G | \Phi \rangle}{\langle \Phi | \hat{P}_G^{\dagger} \hat{P}_G | \Phi \rangle} , \quad (60)$$

and the densities become

$$n_{\sigma}(\mathbf{r}) = \sum_{\mathbf{R},b,\mathbf{R}',b'} \phi_{\mathbf{R},b,\sigma}^*(\mathbf{r}) \phi_{\mathbf{R}',b',\sigma}(\mathbf{r}) \rho_{(\mathbf{R}',b'),(\mathbf{R},b);\sigma}^G . \quad (61)$$

The expectation values for the atomic operators are given by

$$m_{\mathbf{R};\Gamma,\Gamma'}^G = \frac{\langle \Psi_G | \hat{m}_{\mathbf{R};\Gamma,\Gamma'} | \Psi_G \rangle}{\langle \Psi_G | \Psi_G \rangle} = \frac{\langle \Phi | \hat{P}_G^{\dagger} \hat{m}_{\mathbf{R};\Gamma,\Gamma'} \hat{P}_G | \Phi \rangle}{\langle \Phi | \hat{P}_G^{\dagger} \hat{P}_G | \Phi \rangle} . \quad (62)$$

The diagrammatic evaluation of $\rho_{(\mathbf{R}',b'),(\mathbf{R},b);\sigma}^G$ and of $m_{\mathbf{R};\Gamma,\Gamma'}^G$ shows that these quantities are functionals of the non-interacting single-particle density matrices $\tilde{\rho}$, see eq. (30), and of the variational parameters $\lambda_{\Gamma,\Gamma'}(\mathbf{R})$. Moreover, it turns out that the local, non-interacting single-particle density matrix $\tilde{C}(\mathbf{R})$ with the elements

$$C_{b,b';\sigma}(\mathbf{R}) \equiv \rho_{(\mathbf{R},b),(\mathbf{R},b');\sigma} \quad (63)$$

plays a prominent role in the Gutzwiller energy functional, in particular, for infinite lattice coordination number. Therefore, we may write

$$E[\{n_{\sigma}(\mathbf{r})\}, \{|\Psi_G\rangle\}] \equiv E^G[\tilde{\rho}, \{\tilde{\lambda}(\mathbf{R})\}, \{n_{\sigma}(\mathbf{r})\}, \{\tilde{C}(\mathbf{R})\}] . \quad (64)$$

In the Lagrange functional we shall impose the relation (63) with the help of the Hermitian Lagrange parameter matrix $\tilde{\eta}$ with entries $\eta_{(\mathbf{R},b),(\mathbf{R},b');\sigma}$. Lastly, for the

analytical evaluation of eq. (64) it is helpful to impose a set of (real-valued) local constraints ($l = 1, 2, \dots, N_{\text{con}}$)

$$g_{l,\mathbf{R}} [\tilde{\lambda}(\mathbf{R}), \tilde{C}(\mathbf{R})] = 0, \quad (65)$$

which we implement with real Lagrange parameters $\Lambda_l(\mathbf{R})$; for explicit expressions, see eqs. (74) and (75).

In the following, we abbreviate $i = (\mathbf{R}, b)$ and $j = (\mathbf{R}', b')$. Consequently, in analogy with Sect. 2.4, we address

$$G_{\text{DFT}}^{\text{G}} \equiv G_{\text{DFT}}^{\text{G}} \left[\tilde{\rho}, \{n_{\sigma}(\mathbf{r})\}, \{\tilde{C}(\mathbf{R})\}, \{\tilde{\lambda}(\mathbf{R})\} \right] \quad (66)$$

as our Lagrange functional,

$$\begin{aligned} G_{\text{DFT}}^{\text{G}} = & E^{\text{G}} \left[\tilde{\rho}, \{\tilde{\lambda}(\mathbf{R})\}, \{n_{\sigma}(\mathbf{r})\}, \{\tilde{C}(\mathbf{R})\} \right] - \sum_{l,m,\sigma} \Omega_{l,m,\sigma} (\tilde{\rho} \cdot \tilde{\rho} - \tilde{\rho})_{m,l,\sigma} \\ & - \sum_{\sigma} \int d\mathbf{r} \kappa_{\sigma}(\mathbf{r}) \left(n_{\sigma}(\mathbf{r}) - \sum_{i,j} \phi_{i,\sigma}^*(\mathbf{r}) \phi_{j,\sigma}(\mathbf{r}) \rho_{j,i;\sigma}^{\text{G}} \right) \\ & + \sum_{l,\mathbf{R}} \Lambda_l(\mathbf{R}) g_{l,\mathbf{R}} - \sum_{\mathbf{R},b,b',\sigma} \eta_{b,b';\sigma}(\mathbf{R}) \left(C_{b',b;\sigma}(\mathbf{R}) - \rho_{(\mathbf{R},b'),(\mathbf{R},b);\sigma} \right), \end{aligned} \quad (67)$$

cf. eq. (34). Here, we took the condition (61) into account using Lagrange parameters $\kappa_{\sigma}(\mathbf{r})$ because the external potential, the Hartree term and the exchange-correlation potential in eq. (58) depend on the densities.

3.2.3. Minimization of the Gutzwiller energy functional. The functional $G_{\text{DFT}}^{\text{G}}$ in eq. (67) has to be minimized with respect to $n_{\sigma}(\mathbf{r})$, $\tilde{C}(\mathbf{R})$, $\tilde{\lambda}(\mathbf{R})$, and $\tilde{\rho}$. The variation with respect to the Lagrange parameters $\kappa_{\sigma}(\mathbf{r})$, $\tilde{\eta}(\mathbf{R})$, $\Lambda_l(\mathbf{R})$, and $\tilde{\Omega}$ gives the constraints (61), (63), (65), and (33), respectively.

- (i) As in the derivation of the exact Schrödinger equation (53), the variation of $G_{\text{DFT}}^{\text{G}}$ with respect to $n_{\sigma}(\mathbf{r})$ generates the single-particle potential,

$$\kappa_{\sigma}(\mathbf{r}) = V_{\sigma}^{\text{H}}(\mathbf{r}), \quad (68)$$

see eqs. (42) and (51).

- (ii) The minimization with respect to $\tilde{C}(\mathbf{R})$ gives

$$\begin{aligned} \eta_{b,b';\sigma}(\mathbf{R}) = & \frac{\partial E^{\text{G}}}{\partial C_{b',b;\sigma}(\mathbf{R})} + \sum_l \Lambda_l(\mathbf{R}) \frac{\partial g_{l,\mathbf{R}}}{\partial C_{b',b;\sigma}(\mathbf{R})} \\ & + \sum_{i,j,\sigma'} \int d\mathbf{r} V_{\sigma'}^{\text{H}}(\mathbf{r}) \phi_{i,\sigma'}^*(\mathbf{r}) \phi_{j,\sigma'}(\mathbf{r}) \frac{\partial \rho_{j,i;\sigma'}^{\text{G}}}{\partial C_{b',b;\sigma}(\mathbf{R})}. \end{aligned} \quad (69)$$

- (iii) The minimization with respect to the Gutzwiller correlation parameters $\tilde{\lambda}(\mathbf{R})$ results in

$$0 = \frac{\partial E^{\text{G}}}{\partial \lambda_{\Gamma,\Gamma'}(\mathbf{R})} + \sum_{l,m,\sigma} \int d\mathbf{r} V_{\sigma}^{\text{H}}(\mathbf{r}) \phi_{l,\sigma}^*(\mathbf{r}) \phi_{m,\sigma}(\mathbf{r}) \frac{\partial \rho_{m,l,\sigma}^{\text{G}}}{\partial \lambda_{\Gamma,\Gamma'}(\mathbf{R})}$$

$$\begin{aligned}
& + \sum_l \Lambda_l(\mathbf{R}) \frac{\partial g_{l,\mathbf{R}}}{\partial \lambda_{\Gamma,\Gamma'}(\mathbf{R})} \\
& = \sum_{l,m,\sigma} h_{l,m;\sigma}^0 \frac{\partial \rho_{m,l,\sigma}^G}{\partial \lambda_{\Gamma,\Gamma'}(\mathbf{R})} + \frac{\partial (V_{\text{loc}}^G - V_{\text{dc}}^G)}{\partial \lambda_{\Gamma,\Gamma'}(\mathbf{R})} + \sum_l \Lambda_l(\mathbf{R}) \frac{\partial g_{l,\mathbf{R}}}{\partial \lambda_{\Gamma,\Gamma'}(\mathbf{R})},
\end{aligned} \tag{70}$$

$$h_{l,m;\sigma}^0 \equiv \int d\mathbf{r} \phi_{l,\sigma}^*(\mathbf{r}) \left(-\frac{\Delta_{\mathbf{r}}}{2m} + U(\mathbf{r}) + V_{\text{Har}}(\mathbf{r}) + v_{\text{H,xc},\sigma}(\mathbf{r}) \right) \phi_{m,\sigma}(\mathbf{r}) \tag{71}$$

for all $\lambda_{\Gamma,\Gamma'}(\mathbf{R})$. Note that, in the case of complex Gutzwiller parameters, we also have to minimize with respect to $(\lambda_{\Gamma,\Gamma'}(\mathbf{R}))^*$. Using these equations we may calculate the Lagrange parameters $\Lambda_l(\mathbf{R})$ that are needed in eq. (69).

- (iv) The minimization of G_{DFT}^G with respect to $\tilde{\rho}$ generates the Landau–Gutzwiller quasi-particle Hamiltonian, see Appendix A.2,

$$\hat{H}_{\text{qp}}^G = \sum_{i,j,\sigma} h_{i,j;\sigma}^G \hat{c}_{i,\sigma}^\dagger \hat{c}_{j,\sigma} \tag{72}$$

with the entries

$$\begin{aligned}
h_{i,j;\sigma}^G & = \frac{\partial E^G}{\partial \rho_{j,i;\sigma}} + \sum_{l,m,\sigma'} \int d\mathbf{r} V_{\sigma'}^{\text{H}}(\mathbf{r}) \phi_{l,\sigma'}^*(\mathbf{r}) \phi_{m,\sigma'}(\mathbf{r}) \frac{\partial \rho_{m,l,\sigma'}^G}{\partial \rho_{j,i;\sigma}} \\
& + \sum_{\mathbf{R},b,b',\sigma'} \eta_{b,b';\sigma'}(\mathbf{R}) \frac{\partial \rho_{(\mathbf{R},b'),(\mathbf{R},b);\sigma'}}{\partial \rho_{j,i;\sigma}} \\
& = \sum_{l,m,\sigma'} h_{l,m;\sigma'}^0 \frac{\partial \rho_{m,l,\sigma'}^G}{\partial \rho_{j,i;\sigma}} + \frac{\partial (V_{\text{loc}}^G - V_{\text{dc}}^G)}{\partial \rho_{j,i;\sigma}} \\
& + \sum_{\mathbf{R},b,b'} \delta_{j,(\mathbf{R},b')} \delta_{i,(\mathbf{R},b)} \eta_{b,b';\sigma}(\mathbf{R}),
\end{aligned} \tag{73}$$

where we used eqs. (58) and (71).

The single-particle state $|\Phi\rangle$ is the ground state of the Hamiltonian (72) from which the single-particle density matrix $\tilde{\rho}$ follows.

The minimization problem outlined in steps (i)–(iv) requires the evaluation of the energy E^G in eq. (58). In particular, the correlated single-particle density matrix $\tilde{\rho}^G$, eq. (60), must be determined.

All equations derived in this section are completely general. They can, at least in principle, be evaluated by means of a diagrammatic expansion method [20, 21, 22]. The leading order of the expansion corresponds to an approximation-free evaluation of expectation values for Gutzwiller wave functions in the limit of high lattice coordination number. This limit will be studied in the rest of this work.

3.3. Gutzwiller density functional for infinite lattice coordination number

For $Z \rightarrow \infty$, the Gutzwiller-correlated single-particle density matrix and the Gutzwiller probabilities for the local occupancies can be calculated explicitly without further approximations. In this section we make no symmetry assumptions (translational invariance, crystal symmetries). Note, however, that the equations do not cover the case of spin-orbit coupling.

3.3.1. Local constraints. As shown in Refs. [8, 23] it is convenient for the evaluation of Gutzwiller wave functions to impose the following (local) constraints

$$\sum_{\Gamma, \Gamma_1, \Gamma_2} \lambda_{\Gamma, \Gamma_1}^*(\mathbf{R}) \lambda_{\Gamma, \Gamma_2}(\mathbf{R}) \langle \hat{m}_{\mathbf{R}; \Gamma_1, \Gamma_2} \rangle_{\Phi} = 1 \quad (74)$$

and

$$\sum_{\Gamma, \Gamma_1, \Gamma_2} \lambda_{\Gamma, \Gamma_1}^*(\mathbf{R}) \lambda_{\Gamma, \Gamma_2}(\mathbf{R}) \langle \hat{m}_{\mathbf{R}; \Gamma_1, \Gamma_2} \hat{c}_{\mathbf{R}, b, \sigma}^{\dagger} \hat{c}_{\mathbf{R}, b', \sigma} \rangle_{\Phi} = \langle \hat{c}_{\mathbf{R}, b, \sigma}^{\dagger} \hat{c}_{\mathbf{R}, b', \sigma} \rangle_{\Phi}, \quad (75)$$

where we abbreviated $\langle \hat{A} \rangle_{\Phi} \equiv \langle \Phi | \hat{A} | \Phi \rangle$. Note that, for complex constraints, the index l in (65) labels real and imaginary parts separately.

3.3.2. Atomic occupancies. In the limit of infinite lattice coordination number, the interaction and double-counting energy can be expressed solely in terms of the local variational parameters $\tilde{\lambda}(\mathbf{R})$ and the local density matrix $\tilde{C}(\mathbf{R})$ of the correlated bands in $|\Phi\rangle$,

$$V_{\text{loc/dc}}^G = \sum_{\mathbf{R}} \sum_{\Gamma_1, \dots, \Gamma_4} \lambda_{\Gamma_2, \Gamma_1}^*(\mathbf{R}) E_{\Gamma_2, \Gamma_3}^{\text{loc/dc}}(\mathbf{R}) \lambda_{\Gamma_3, \Gamma_4}(\mathbf{R}) \langle \hat{m}_{\mathbf{R}; \Gamma_1, \Gamma_4} \rangle_{\Phi}. \quad (76)$$

The remaining expectation values $\langle \hat{m}_{\mathbf{R}; \Gamma_1, \Gamma_4} \rangle_{\Phi}$ are evaluated using Wick's theorem. Explicit expressions are given in Refs. [8, 24].

3.3.3. Correlated single-particle density matrix. The local part of the correlated single-particle density matrix is given by

$$\begin{aligned} \rho_{(\mathbf{R}', b'), (\mathbf{R}, b); \sigma}^G &= \sum_{\Gamma_1, \dots, \Gamma_4} \lambda_{\Gamma_2, \Gamma_1}^*(\mathbf{R}) \lambda_{\Gamma_3, \Gamma_4}(\mathbf{R}) \langle \hat{m}_{\mathbf{R}; \Gamma_1, \Gamma_2} \hat{c}_{\mathbf{R}, b, \sigma}^{\dagger} \hat{c}_{\mathbf{R}, b', \sigma} \hat{m}_{\mathbf{R}; \Gamma_3, \Gamma_4} \rangle_{\Phi} \\ &\equiv C_{b', b; \sigma}^G(\mathbf{R}). \end{aligned} \quad (77)$$

It can be evaluated using Wick's theorem. As can be seen from eq. (77), it is a function of the variational parameters $\lambda_{\Gamma, \Gamma'}(\mathbf{R})$ and of the local non-interacting single-particle density matrix $\tilde{C}(\mathbf{R})$.

For $\mathbf{R} \neq \mathbf{R}'$, we have for the correlated single-particle density matrix

$$\rho_{(\mathbf{R}', b'), (\mathbf{R}, b); \sigma}^G = \sum_{a, a'} q_{b, \sigma}^{a, \sigma}(\mathbf{R}) \left(q_{b', \sigma}^{a', \sigma}(\mathbf{R}') \right)^* \rho_{(\mathbf{R}', a'), (\mathbf{R}, a); \sigma} \quad (78)$$

with the orbital-dependent renormalization factors $q_{b, \sigma}^{a, \sigma}(\mathbf{R})$ for the electron transfer between different sites. Explicit expressions in terms of the variational parameters $\tilde{\lambda}(\mathbf{R})$ and of the local non-interacting single-particle density matrix $\tilde{C}(\mathbf{R})$ are given in Refs. [8, 24].

4. Implementation for translational invariant systems

For a system that is invariant under translation by a lattice vector and contains only one atom per unit cell, all local quantities become independent of the site index, e.g., $\lambda_{\Gamma, \Gamma'}(\mathbf{R}) \equiv \lambda_{\Gamma, \Gamma'}$ for the Gutzwiller variational parameters. Since \mathbf{k} from the first

Brillouin zone is a good quantum number, we work with the (orbital) Bloch basis, see Appendix A.3. It is straightforward to generalize the equations in Sect. 4 to the case of more than one atom per unit cell. One simply has to add one more index that labels the atoms in the unit cell.

As shown in Sect. 3.2.3, the minimization of the Gutzwiller energy functional requires two major steps, namely, the variation with respect to the Gutzwiller parameters $\tilde{\lambda}$ and the variation with respect to the single-particle density matrix $\tilde{\rho}$ that characterizes the single-particle product state $|\Phi\rangle$.

4.1. Gutzwiller–Kohn–Sham Hamiltonian

The minimization of the energy functional with respect to the single-particle density matrix leads to the Gutzwiller–Kohn–Sham Hamiltonian. In the orbital Bloch basis $\phi_{\mathbf{k},b,\sigma}(\mathbf{r})$, see Appendix A.3, the corresponding quasi-particle Hamiltonian reads

$$\hat{H}_{\text{qp}}^{\text{G}} = \sum_{\mathbf{k},b,b',\sigma} h_{b,b';\sigma}^{\text{G}}(\mathbf{k}) \hat{c}_{\mathbf{k},b,\sigma}^{\dagger} \hat{c}_{\mathbf{k},b',\sigma}, \quad (79)$$

see eq. (72). In this section, we shall explain how this Hamiltonian can be calculated. Note, however, that the actual numerical implementation within QUANTUMESPRESSO is done in first quantization and uses plane-waves. We therefore derive the plane-wave representation of the Gutzwiller–Kohn–Sham equations in Appendix B.

4.1.1. Derivation of matrix elements. When we apply the general expressions (73), the matrix elements of the quasi-particle Hamiltonian are obtained as

$$h_{b,b';\sigma}^{\text{G}}(\mathbf{k}) = \eta_{b,b';\sigma} + \sum_{a,a',\sigma'} h_{a,a';\sigma'}^0(\mathbf{k}) \frac{\partial \rho_{a',a;\sigma'}^{\text{G}}(\mathbf{k})}{\partial \rho_{b',b;\sigma}(\mathbf{k})}, \quad (80)$$

where we have from eq. (71)

$$h_{a,a';\sigma}^0(\mathbf{k}) = \int d\mathbf{r} \phi_{\mathbf{k},a,\sigma}^*(\mathbf{r}) \left(-\frac{\Delta \mathbf{r}}{2m} + U(\mathbf{r}) + V_{\text{Har}}(\mathbf{r}) + v_{\text{H,xc},\sigma}(\mathbf{r}) \right) \phi_{\mathbf{k},a',\sigma}(\mathbf{r}). \quad (81)$$

Moreover,

$$\rho_{b',b;\sigma}(\mathbf{k}) = \langle \Phi | \hat{c}_{\mathbf{k},b,\sigma}^{\dagger} \hat{c}_{\mathbf{k},b',\sigma} | \Phi \rangle \quad (82)$$

are the entries of the single-particle density matrix in the orbital Bloch basis, and $\rho_{b',b;\sigma}^{\text{G}}(\mathbf{k})$ denotes the corresponding quantities in the Gutzwiller-correlated state. In the limit of infinite lattice coordination number, we may express $V_{\text{loc/dc}}^{\text{G}}$ in eq. (73) as a function of the Gutzwiller variational parameters $\lambda_{\Gamma,\Gamma'}$ and of the local density matrix \tilde{C} . Therefore, $V_{\text{loc/dc}}^{\text{G}}$ are formally independent of the single-particle density matrix $\tilde{\rho}$ so that they do not contribute to $h_{b,b';\sigma}^{\text{G}}(\mathbf{k})$. Equation (80) shows that, apart from an overall shift of the orbitals through $\eta_{b,b';\sigma}$, we can still work with the matrix elements $h_{a,a';\sigma'}^0(\mathbf{k})$ of the single-particle operator \hat{H}_0 that enters the many-particle Schrödinger equation (53).

In the orbital Bloch basis, eqs. (77) and (78) take the form

$$\rho_{b',b;\sigma}^G(\mathbf{k}) = \sum_{a,a'} q_{b,\sigma}^{a,\sigma} \left(q_{b',\sigma}^{a',\sigma} \right)^* (\rho_{a',a;\sigma}(\mathbf{k}) - C_{a',a;\sigma}) + C_{b',b;\sigma}^G. \quad (83)$$

When we insert eq. (83) into eq. (80) we thus find for the entries of the Gutzwiller quasi-particle Hamiltonian

$$h_{b,b';\sigma}^G(\mathbf{k}) = \eta_{b,b';\sigma} + \sum_{a,a'} q_{a,\sigma}^{b,\sigma} \left(q_{a',\sigma}^{b',\sigma} \right)^* h_{a,a';\sigma}^0(\mathbf{k}). \quad (84)$$

Recall that the local single-particle densities \tilde{C} are treated as independent parameters. Since the q -factors and the correlated local single-particle density matrix $C_{b,b';\sigma}^G = \rho_{(\mathbf{R},b),(\mathbf{R},b');\sigma}^G$ are solely functions of the variational parameters $\tilde{\lambda}$ and of \tilde{C} , they are treated as constants when we take the derivative of $\rho_{b',b;\sigma}^G(\mathbf{k})$ with respect to $\rho_{b',b;\sigma}(\mathbf{k})$ in eq. (83).

4.1.2. Diagonalization of the quasi-particle Hamiltonian. The unitary matrix $\tilde{F}_\sigma^G(\mathbf{k})$ diagonalizes the Gutzwiller matrix $\tilde{h}_\sigma^G(\mathbf{k})$,

$$\sum_{b,b'} (F_{b,n,\sigma}^G(\mathbf{k}))^* h_{b,b';\sigma}^G(\mathbf{k}) F_{b',m,\sigma}^G(\mathbf{k}) = \delta_{n,m} \epsilon_{n,\sigma}^G(\mathbf{k}), \quad (85)$$

which provides the quasi-particle dispersion $\epsilon_{n,\sigma}^G(\mathbf{k})$. We introduce the quasi-particle band operators

$$\hat{g}_{\mathbf{k},n,\sigma}^\dagger = \sum_b F_{b,n,\sigma}^G(\mathbf{k}) \hat{c}_{\mathbf{k},b,\sigma}^\dagger, \quad \hat{g}_{\mathbf{k},n,\sigma} = \sum_b (F_{b,n,\sigma}^G(\mathbf{k}))^* \hat{c}_{\mathbf{k},b,\sigma}, \quad (86)$$

in which the Gutzwiller quasi-particle Hamiltonian becomes diagonal,

$$\hat{H}_{\text{qp}}^G = \sum_{\mathbf{k},n,\sigma} \epsilon_{n,\sigma}^G(\mathbf{k}) \hat{g}_{\mathbf{k},n,\sigma}^\dagger \hat{g}_{\mathbf{k},n,\sigma}. \quad (87)$$

In order to minimize the Gutzwiller density functional G_{DFT}^G , we must work with the ground state of the quasi-particle Hamiltonian \hat{H}_{qp}^G ,

$$|\Phi_0\rangle = \prod_{\mathbf{k},n,\sigma} ' \hat{g}_{\mathbf{k},n,\sigma}^\dagger |\text{vac}\rangle, \quad (88)$$

where the N levels lowest in energy are occupied as indicated by the prime at the product, $\epsilon_{n,\sigma}^G(\mathbf{k}) \leq E_{\text{F},\sigma}^G$. Using eq. (82) we find

$$\begin{aligned} \rho_{b',b;\sigma}^{\text{opt}}(\mathbf{k}) &= \langle \hat{c}_{\mathbf{k},b,\sigma}^\dagger \hat{c}_{\mathbf{k},b',\sigma} \rangle_{\Phi_0} \\ &= \sum_n (F_{b,n,\sigma}^G(\mathbf{k}))^* F_{b',n,\sigma}^G(\mathbf{k}) \langle \hat{g}_{\mathbf{k},n,\sigma}^\dagger \hat{g}_{\mathbf{k},n,\sigma} \rangle_{\Phi_0} \\ &= \sum_n f_{\mathbf{k},n,\sigma}^G (F_{b,n,\sigma}^G(\mathbf{k}))^* F_{b',n,\sigma}^G(\mathbf{k}), \end{aligned} \quad (89)$$

where the quasi-particle occupancies

$$f_{\mathbf{k},n,\sigma}^G = \langle \hat{g}_{\mathbf{k},n,\sigma}^\dagger \hat{g}_{\mathbf{k},n,\sigma} \rangle_{\Phi_0} = \Theta(E_{\text{F},\sigma}^G - \epsilon_{n,\sigma}^G(\mathbf{k})) \quad (90)$$

are unity for occupied quasi-particle levels up to the Fermi energy $E_{\text{F},\sigma}^G$, and zero otherwise. The particle densities follow from eq. (89),

$$n_\sigma(\mathbf{r}) = \sum_{\mathbf{k},b,b'} \phi_{\mathbf{k},b,\sigma}^*(\mathbf{r}) \phi_{\mathbf{k},b',\sigma}(\mathbf{r}) \rho_{b',b;\sigma}^G(\mathbf{k}), \quad (91)$$

where $\rho_{b',b;\sigma}^G(\mathbf{k})$ is given by eq. (83). As in DFT, the particle densities must be calculated self-consistently.

4.1.3. Band-shift parameters. In order to determine the band-shift parameters $\eta_{b,b';\sigma}$, we must evaluate eq. (69) using the Gutzwiller energy functional in the limit of infinite lattice coordination number. We define the kinetic energy of the Gutzwiller quasi-particles as

$$E_{\text{kin}}^G = \sum_{\mathbf{k},n,\sigma} f_{\mathbf{k},n,\sigma}^G \epsilon_{n,\sigma}^G(\mathbf{k}) = \sum_{\mathbf{k},b,b',\sigma} h_{b,b';\sigma}^G(\mathbf{k}) \rho_{b',b;\sigma}^G(\mathbf{k}) . \quad (92)$$

It is easy to show that

$$\begin{aligned} \sum_{\mathbf{k},b,b',\sigma} h_{b,b';\sigma}^0(\mathbf{k}) \rho_{b',b;\sigma}^G(\mathbf{k}) &= E_{\text{kin}}^G - \sum_{\mathbf{k},b,b',\sigma} \eta_{b,b';\sigma} \rho_{b',b;\sigma}^G(\mathbf{k}) \\ &\quad + L \sum_{b,b',\sigma} h_{b,b';\sigma}^0 \left(C_{b',b;\sigma}^G - C_{b',b;\sigma} \right) , \\ h_{b,b';\sigma}^0 &= \frac{1}{L} \sum_{\mathbf{k}} h_{b,b';\sigma}^0(\mathbf{k}) . \end{aligned} \quad (93)$$

Then, eq. (69) gives the effective local hybridizations $\eta_{b,b';\sigma}$

$$\begin{aligned} L\eta_{b,b';\sigma} &= \frac{\partial}{\partial C_{b',b;\sigma}^G} \left(L \sum_l \Lambda_l g_l + V_{\text{loc}}^G - V_{\text{dc}}^G + E_{\text{kin}}^G \right. \\ &\quad \left. + L \sum_{a,a',\sigma'} \left(C_{a',a;\sigma}^G - C_{a',a;\sigma} \right) h_{a,a';\sigma'}^0 \right) . \end{aligned} \quad (94)$$

Note that the term in the second line in eq. (94) often vanishes due to symmetry, e.g., in nickel, because $C_{b,b';\sigma}^G = C_{b,b';\sigma}$.

4.2. Minimization with respect to the Gutzwiller parameters

In the ('inner') minimization with respect to the Gutzwiller parameters $\lambda_{\Gamma,\Gamma'}$ (which are now independent of \mathbf{R}) we assume that the single-particle state $|\Phi\rangle$ is fixed. Then we have to minimize the function

$$\begin{aligned} E^{\text{inner}}(\tilde{\lambda}, \{\Lambda_l\}) &\equiv \sum_{\Gamma_1, \dots, \Gamma_4} \lambda_{\Gamma_2, \Gamma_1}^* (E_{\Gamma_2, \Gamma_3}^{\text{loc}} - E_{\Gamma_2, \Gamma_3}^{\text{dc}}) \lambda_{\Gamma_3, \Gamma_4} \langle \hat{m}_{\Gamma_1, \Gamma_4} \rangle_{\Phi} \\ &\quad + \sum_{\sigma} \sum_{c_1, c_2} \left[\sum_{c_3, c_4} q_{c_1, \sigma}^{c_2, \sigma}(\tilde{\lambda}) \left(q_{c_3, \sigma}^{c_4, \sigma}(\tilde{\lambda}) \right)^* I_{c_1, c_3, c_2, c_4}^{\sigma} + \left(q_{c_2, \sigma}^{c_1, \sigma}(\tilde{\lambda}) K_{c_1, c_2}^{\sigma} + \text{c.c.} \right) \right] \\ &\quad + \sum_{\sigma} \sum_{b, b'} h_{b,b';\sigma}^0 C_{b',b;\sigma}^G(\tilde{\lambda}) + \sum_l \Lambda_l g_l(\tilde{\lambda}) , \end{aligned} \quad (95)$$

where we introduced

$$I_{c_1, c_3, c_2, c_4}^{\sigma} \equiv \frac{1}{L} \sum_{\mathbf{k}} h_{c_1, c_3; \sigma}^0(\mathbf{k}) (\rho_{c_4, c_2; \sigma}(\mathbf{k}) - C_{c_4, c_2; \sigma}) , \quad (96)$$

$$K_{c, c'}^{\sigma} \equiv \frac{1}{L} \sum_{\mathbf{k}} \sum_{\bar{c}, \bar{c}'} h_{c, \bar{c}; \sigma}^0(\mathbf{k}) (\rho_{\bar{c}', c'; \sigma}(\mathbf{k}) - C_{\bar{c}', c'; \sigma}) . \quad (97)$$

Here, the indices c and \bar{c} denote correlated and non-correlated orbitals, respectively. Note that the sum over b, b' in the last line of eq. (95) only contributes in the minimization if (at least) one of these two indices belongs to a correlated orbital. An efficient algorithm for the minimization of (95) has been introduced in Ref. [24]. This minimization also gives us the Lagrange parameters Λ_l that enter the outer minimization in eq. (94).

5. Results for ferromagnetic nickel

5.1. Local Hamiltonian and double-counting corrections

For a Gutzwiller DFT calculation we need to specify the Coulomb parameters in the local Hamiltonian (44) and the form of the double-counting operator in (43).

5.1.1. Cubic symmetry and spherical approximation. In many theoretical studies one uses a Hamiltonian with only density-density interactions,

$$\hat{V}_{\text{loc}}^{\text{dens}} = \sum_{c,\sigma} U(c, c) \hat{n}_{c,\sigma} \hat{n}_{c,\bar{\sigma}} + \sum_{c(\neq)c'} \sum_{\sigma,\sigma'} \tilde{U}_{\sigma,\sigma'}(c, c') \hat{n}_{c,\sigma} \hat{n}_{c',\sigma'}. \quad (98)$$

Here, we introduced $\bar{\uparrow} = \downarrow$ ($\bar{\downarrow} = \uparrow$) and $\tilde{U}_{\sigma,\sigma'}(c, c') = U(c, c') - \delta_{\sigma,\sigma'} J(c, c')$, where $U(c, c')$ and $J(c, c')$ are the local Hubbard and Hund's-rule exchange interactions. An additional and quite common approximation is the use of orbital-independent Coulomb parameters,

$$U(c, c) \equiv U, \quad \text{and} \quad U(c, c') \equiv U', \quad J(c, c') \equiv J \quad \text{for } c \neq c'. \quad (99)$$

For a system of five correlated $3d$ orbitals in a cubic environment as in nickel, however, the Hamiltonian (98) is incomplete [25]. The full Hamiltonian reads

$$\hat{V}_{\text{loc}}^{\text{full}} = \hat{V}_{\text{loc}}^{\text{dens}} + \hat{V}_{\text{loc}}^{\text{n.dens.}}, \quad (100)$$

where

$$\begin{aligned} \hat{V}_{\text{loc}}^{\text{n.dens.}} = & \sum_{c(\neq)c'} J(c, c') \left(\hat{c}_{c,\uparrow}^\dagger \hat{c}_{c,\downarrow}^\dagger \hat{c}_{c',\downarrow} \hat{c}_{c',\uparrow} + \text{h.c.} \right) + \sum_{c(\neq)c';\sigma} J(c, c') \hat{c}_{c,\sigma}^\dagger \hat{c}_{c',\bar{\sigma}}^\dagger \hat{c}_{c,\bar{\sigma}} \hat{c}_{c',\sigma} \\ & + \left[\sum_{t;\sigma,\sigma'} (T(t) - \delta_{\sigma,\sigma'} A(t)) \hat{n}_{t,\sigma} \hat{c}_{u,\sigma'}^\dagger \hat{c}_{v,\sigma'} \right. \\ & + \sum_{t,\sigma} A(t) \left(\hat{c}_{t,\sigma}^\dagger \hat{c}_{t,\bar{\sigma}}^\dagger \hat{c}_{u,\bar{\sigma}} \hat{c}_{v,\sigma} + \hat{c}_{t,\sigma}^\dagger \hat{c}_{u,\bar{\sigma}}^\dagger \hat{c}_{t,\bar{\sigma}} \hat{c}_{v,\sigma} \right) \\ & \left. + \sum_{t(\neq)t'(\neq)t''} \sum_{e,\sigma,\sigma'} S(t, t'; t'', e) \hat{c}_{t,\sigma}^\dagger \hat{c}_{t',\sigma'}^\dagger \hat{c}_{t'',\sigma'} \hat{c}_{e,\sigma} + \text{h.c.} \right]. \quad (101) \end{aligned}$$

Here, $t = \zeta, \eta, \xi$ and $e = u, v$ are indices for the three t_{2g} orbitals with symmetries $\zeta = xy$, $\eta = xz$, and $\xi = yz$, and the two e_g orbitals with symmetries $u = 3z^2 - r^2$ and $v = x^2 - y^2$, respectively. The parameters $A(t)$, $T(t)$, $S(t, t'; t'', e)$ in eq. (101) are of the same order of magnitude as the exchange interactions $J(c, c')$ and, hence, there is no a-priori reason to neglect $\hat{V}_{\text{loc}}^{\text{n.dens.}}$. Of all the parameters $U(c, c')$, $J(c, c')$, $A(t)$, $T(t)$, $S(t, t'; t'', e)$ only ten are independent in cubic symmetry, see Appendix C.

When we assume that all 3d-orbitals have the same radial wave-function (‘spherical approximation’), all parameters are determined by, e.g., the three Racah parameters A, B, C . For comparison with other work, we introduce the average Coulomb interaction between electrons in the same 3d-orbitals, $U = \sum_c U(c, c)/5 = A + 4B + 3C$, the average Coulomb interaction between electrons in different orbitals, $U' = \sum_{c < c'} U(c, c')/10 = A - B + C$, and the average Hund’s-rule exchange interaction, $J = \sum_{c < c'} J(c, c')/10 = 5B/2 + C$ that are related by the symmetry relation $U' = U - 2J$, see Appendix C. Due to this symmetry relation, the three values of U , U' , and J do not determine the Racah parameters A, B, C uniquely. Therefore, we make use of the relation $C/B = 4$ which is a reasonable assumption for metallic nickel [8, 25]. In this way, the three Racah parameters and, consequently, all parameters in $\hat{V}_{\text{loc}}^{\text{full}}$ are functions of U and J , $A = U - 32J/13$, $B = 2J/13$, $C = 8J/13$. This permits a meaningful comparison of our results for all local Hamiltonians. Later we shall compare our results for $\hat{V}_{\text{loc}}^{\text{dens}}$ with orbital-independent values for U , U' and $J = (U - U')/2$, see eq. (99), with those for the full local Hamiltonian, $\hat{V}_{\text{loc}}^{\text{full}}$, for the same values for U and J .

5.1.2. Double counting corrections. There exists no systematic (let alone rigorous) derivation of the double-counting correction in eq. (43). A widely used form for this operator has first been introduced in the context of the LDA+ U method. Its expectation value is given by

$$V_{\text{dc};1}^{\text{G}} = \frac{U}{2} \bar{n}(\bar{n} - 1) - \frac{J}{2} \sum_{\sigma} \bar{n}_{\sigma}(1 - \bar{n}_{\sigma}) , \quad (102)$$

where $\bar{n}_{\sigma} \equiv \sum_{c=1}^{N_c} C_{c,c;\sigma}^{\text{G}}$, $\bar{n} \equiv \bar{n}_{\uparrow} + \bar{n}_{\downarrow}$, and N_c is the number of correlated orbitals ($N_c = 5$ for nickel). Note that only the two mean values U and J enter this double-counting operator, i.e., it is the same for all local Hamiltonians introduced above.

The physical consequences of the double-counting correction are most pronounced in its impact on the local energy-shifts $\eta_{c,c;\sigma}$ which we may write as

$$\eta_{c,c;\sigma} \equiv \eta_{c,c;\sigma}^{\text{G}} - \eta_{c,c;\sigma}^{\text{dc}} , \quad \eta_{c,c;\sigma}^{\text{dc}} = \frac{\partial V_{\text{dc}}^{\text{G}}}{\partial C_{c,c;\sigma}} . \quad (103)$$

For nickel, the cubic symmetry guarantees that

$$C_{c,c';\sigma}^{\text{G}} = C_{c,c';\sigma} = \delta_{c,c'} C_{c,c;\sigma} , \quad (104)$$

i.e., the correlated and uncorrelated local densities agree with each other. The double-counting correction (102) leads to $\eta_{c,c;\sigma}^{\text{dc},1} = U(\bar{n} - 1/2) + J(\bar{n}_{\sigma} - 1/2)$. It has been argued in Ref. [11] that this double-counting correction is insufficient for the investigation of cerium and some of its compounds. Instead, the authors of that work propose two alternative double-counting corrections which, in effect, correspond to the energy shifts

$$V_{\text{dc};2}^{\text{G}} : \eta_{c,c;\sigma}^{\text{dc},2} = \eta_{c,c;\sigma}^{\text{G}} \quad \text{so that } \eta_{c,c;\sigma} \equiv 0 , \quad (105)$$

$$V_{\text{dc};3}^{\text{G}} : \eta_{c,c;\sigma}^{\text{dc},3} = \frac{1}{N_c} \sum_c \eta_{c,c;\sigma}^{\text{G}} . \quad (106)$$

As we will demonstrate in the following section, these three double-counting corrections lead to noticeably different results for nickel. This is a rather unsatisfactory observation because it compromises the predictive power of the method if the results strongly depend on the particular choice of the double-counting correction. In Ref. [26] a scheme has been proposed which does not rely on the subtraction of double-counting operators and instead addresses the density functional directly. It needs to be seen if this method can provide a more general way to tackle the double-counting problem within the Gutzwiller DFT.

5.2. Implementation in DFT

We implemented our Gutzwiller scheme in the QUANTUMESPRESSO DFT code; for details on QUANTUMESPRESSO, see Ref. [27].

Due to the cubic symmetry of nickel, the single-particle density matrix \tilde{C} is diagonal with the local occupancies $C_{t;\sigma} \equiv C_{\xi,\xi;\sigma} = C_{\eta,\eta;\sigma} = C_{\zeta,\zeta;\sigma}$ in the t_{2g} -orbitals and $C_{e;\sigma} \equiv C_{u,u;\sigma} = C_{v,v;\sigma}$ in the e_g -orbitals. Likewise, the matrix $\tilde{\eta}$ is diagonal with the corresponding entries $\eta_{t;\sigma}$ and $\eta_{e;\sigma}$. Moreover, the q -matrix is diagonal, $q_{a,\sigma}^{b,\sigma} = \delta_{a,b} q_{a,\sigma}$ with identical entries for the three t_{2g} -orbitals, $q_{\xi,\sigma} = q_{\eta,\sigma} = q_{\zeta,\sigma} \equiv q_{t,\sigma}$, and the two e_g -orbitals, $q_{u,\sigma} = q_{v,\sigma} \equiv q_{e,\sigma}$, respectively. Formulae for $q_{t,\sigma}$ and $q_{e,\sigma}$ as a function of the Gutzwiller parameters $\tilde{\lambda}$ and of $C_{e;\sigma}$ and $C_{t;\sigma}$ are given in Refs. [8, 24].

5.2.1. Setup: DFT calculation and Wannier orbitals. As a first step, we perform a DFT calculation that corresponds to setting $U = J = 0$. We use the LDA exchange-correlation potential,

$$v_{\text{H,xc},\sigma}(\mathbf{r}) = \left. \frac{\partial E_{\text{LDA,xc}}[\{n_\sigma(\mathbf{r})\}]}{\partial n_\sigma(\mathbf{r})} \right|_{n_\sigma(\mathbf{r})=n_\sigma^0(\mathbf{r})}, \quad (107)$$

see eq. (52), as implemented in QUANTUMESPRESSO. The Kohn-Sham equations are solved in the plane-wave basis using ultra-soft pseudo-potentials, see eq. (A.23). This calculation provides the Kohn-Sham bandstructure $\epsilon_{\mathbf{n},\sigma}(\mathbf{k})$ and the coefficients $C_{\mathbf{G},\mathbf{n},\sigma}(\mathbf{k}) = \langle \mathbf{k}, \mathbf{G}, \sigma | \mathbf{k}, \mathbf{n}, \sigma \rangle$ of the Kohn-Sham eigenstates $\psi_{\mathbf{k},\mathbf{n},\sigma}(\mathbf{r})$ in the plane-wave basis. The implemented ‘poor-man Wannier’ program package provides the down-folded 3d Wannier orbitals $\phi_{\mathbf{R},c,\sigma}(\mathbf{r})$. In the orbital Bloch basis the coefficients $\langle \mathbf{k}, \mathbf{G}, \sigma | \mathbf{k}, c, \sigma \rangle$ describe $\phi_{\mathbf{k},c,\sigma}(\mathbf{r})$ in the plane-wave basis.

5.2.2. Gutzwiller–Kohn–Sham loop. At the beginning we set $q_{a,\sigma}^{b,\sigma} = \delta_{a,b}$ and $\tilde{\eta} = 0$. Our Gutzwiller–Kohn–Sham loop consists of the following steps.

- (i) Perform a DFT calculation with the Gutzwiller Kohn–Sham Hamiltonian from eq. (B.11), and the Gutzwiller Kohn–Sham densities from eq. (B.5). Here, the form $Q_{\mathbf{G},\mathbf{G}';\sigma}(\mathbf{k}) = \delta_{\mathbf{G},\mathbf{G}'} + \sum_c (q_c - 1) \langle \mathbf{k}, \mathbf{G}, \sigma | \mathbf{k}, c, \sigma \rangle \langle \mathbf{k}, c, \sigma | \mathbf{k}, \mathbf{G}', \sigma \rangle$ is useful where only the correlated orbitals appear explicitly.

After reaching a self-consistent density $n_\sigma(\mathbf{r})$, calculate the local single-particle density matrix,

$$C_{c,c;\sigma} = \frac{1}{L} \sum_{\mathbf{k},n} f_{\mathbf{k},n,\sigma} \sum_{\mathbf{G},\mathbf{G}'} \langle \mathbf{k}, n, \sigma | \mathbf{k}, \mathbf{G}, \sigma \rangle \langle \mathbf{k}, \mathbf{G}, \sigma | \mathbf{k}, c, \sigma \rangle \langle \mathbf{k}, c, \sigma | \mathbf{k}, \mathbf{G}', \sigma \rangle \langle \mathbf{k}, \mathbf{G}', \sigma | \mathbf{k}, n, \sigma \rangle, \quad (108)$$

and the quantities $I_{c_1,c_3,c_2,c_4}^\sigma$ from eq. (96) and $K_{c,c'}^\sigma$ from eq. (97). For a proper convergence of the Gutzwiller–Kohn–Sham loop these quantities must be calculated with a momentum-space resolution that exceeds that of an ordinary DFT calculation considerably. To achieve this goal we use a tetrahedron method with 826 \mathbf{k} -points in the symmetry-reduced Brillouin zone.

- (ii) Perform the inner minimization, i.e., minimize the energy functional E^{inner} in eq. (95). This step provides the values for the Lagrange parameters Λ_l and for the Gutzwiller variational parameters $\tilde{\lambda}$ that determine the orbital-dependent renormalization factors $q_{c,\sigma}$ in eq. (78).
- (iii) Calculate the entries of $\tilde{\eta}$ from eq. (94).
- (iv) If the total energy does not decrease compared with the previous iteration, the calculation has converged and the loop terminates. If not, repeat the loop starting at step (i).

The steps (ii) and (iii) are carried out following the algorithm outlined previously [24].

In the present version of the program, step (i) requires a full DFT calculation which, however, is numerically cheap for the simple nickel system. In the future, we plan to include the Gutzwiller minimization directly in the DFT minimization cycle.

The Gutzwiller approach permits the definition of correlated orbital Bloch states, see Appendix B. Therefore, we can compare our original $3d$ Wannier orbitals with the Gutzwiller correlated Wannier orbitals. For nickel, we find that the deviations are negligibly small. In general, we may include the correlation-induced shape changes of the correlated Wannier orbitals in our self-consistent calculations.

5.3. Results

The electronic properties of nickel have already been investigated by means of Gutzwiller wave functions in Refs. [12, 13, 14]. In these works we started from a paramagnetic DFT-LDA calculation that provided the band parameters for a tight-binding model. In order to overcome the deficiencies in the underlying DFT-LDA results, we fixed the magnetic moment and other single-particle properties at their experimental values. As we will show in this section, the Gutzwiller DFT mends most of the DFT-LDA shortcomings.

As a variational approach, the Gutzwiller DFT is expected to be most suitable for the calculation of ground-state properties such as the lattice constant, the magnetic moment, or the Fermi surface of a Fermi liquid. Although more speculative than the ground-state calculations, it is also common to interpret the eigenvalues of the Gutzwiller–Kohn–Sham Hamiltonian $\epsilon_{n,\sigma}^G(\mathbf{k})$ as the dispersion of the single-particle

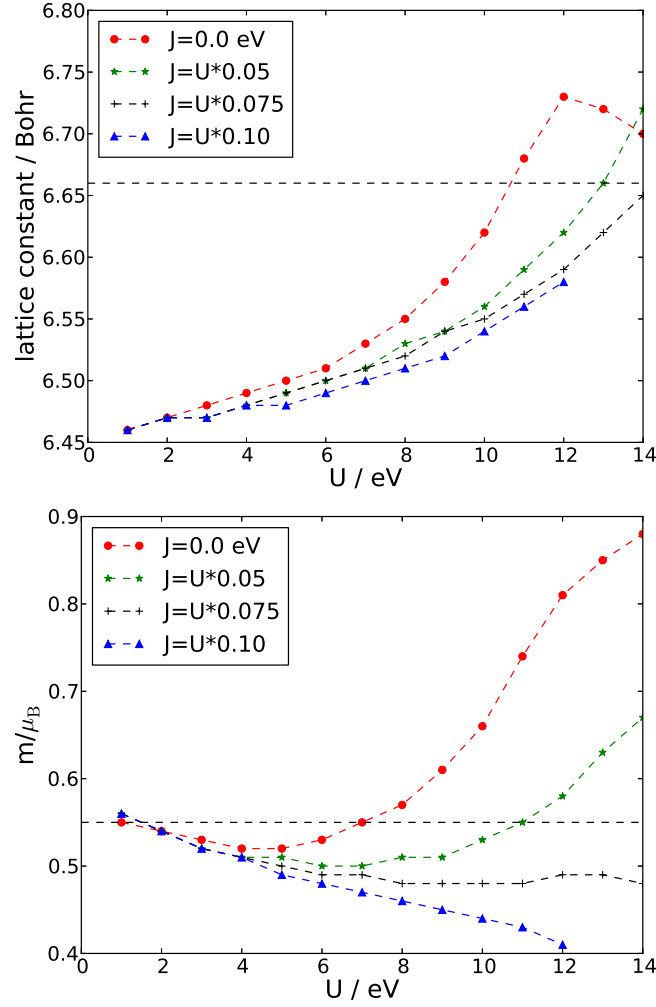


Figure 1. Lattice constant (top) and magnetic moment (bottom) of nickel as a function of U , for four different values of J/U , calculated with the full local Hamiltonian $\hat{V}_{\text{loc}}^{\text{full}}$ and the double counting correction $\hat{V}_{\text{dc};1}$; dashed lines: experimental values.

excitations [28]. We shall discuss our results for the ground-state properties and single-particle excitations separately.

5.3.1. Lattice constant, magnetic moment, and bulk modulus of nickel. In Fig. 1, we show the lattice constant and the magnetic moment as a function of U ($1 \text{ eV} \leq U \leq 14 \text{ eV}$) for four different values of J/U ($J/U = 0, 0.05, 0.075, 0.10$). In these calculations we used the full local Hamiltonian $\hat{V}_{\text{loc}}^{\text{full}}$ and the double-counting correction $\hat{V}_{\text{dc};1}$.

As is well known, the DFT-LDA underestimates the lattice constant. We obtain $a_0^{\text{LDA}} = 6.47a_B$, considerably smaller than the experimental value of $a_0 = 6.66a_B$ where $a_B = 0.529177 \text{ \AA}$ is the Bohr radius. Fig. 1 shows that the Hubbard interaction U increases the lattice constant whereby the Hund's-rule exchange J diminishes the slope. Apparently, a good agreement with the experimental lattice constant requires substantial Hubbard interactions, $U > 10 \text{ eV}$.

Fig. 1 shows the well-known fact that DFT-LDA reproduces the experimental value for the spin-only magnetic moment m_{so} very well, $m_{\text{so}}^{\text{LDA}} = 0.58\mu_{\text{B}}$ vs. $m_{\text{so}}^{\text{exp}} = 0.55\mu_{\text{B}}$. However, when the DFT-LDA calculation is performed for the experimental value of the lattice constant, the magnetic moment is grossly overestimated. As seen in Fig. 1, the Gutzwiller DFT allows us to reconcile the experimental findings both for the lattice constant and the magnetic moment if we work in the parameter range $11\text{ eV} < U < 14\text{ eV}$ and $0.05 < J/U < 0.07$. Note that a ‘fine-tuning’ of parameters is not required to obtain a reasonable agreement between theory and experiment for the lattice constant and spin-only magnetic moment.

Our effective values are chosen to fit the experimental data for the lattice constant and the magnetic moment. The size of U and J agrees with those used in previous Gutzwiller-DFT studies on nickel [10, 12, 13, 14]. For the Gutzwiller-DFT the Hubbard- U lies between the bare, atomic value $U_{\text{bare}} \approx 25\text{ eV}$ [29] and the low-frequency value for the screened on-site interaction $U_{\text{LDA+RPA}}(\omega \rightarrow 0) \approx 4\text{ eV}$, as obtained from LDA+Random-Phase Approximation [30] and used in LDA+DMFT [31]. This comparison shows that the Gutzwiller-DFT works with a partly screened value for the Hubbard interaction.

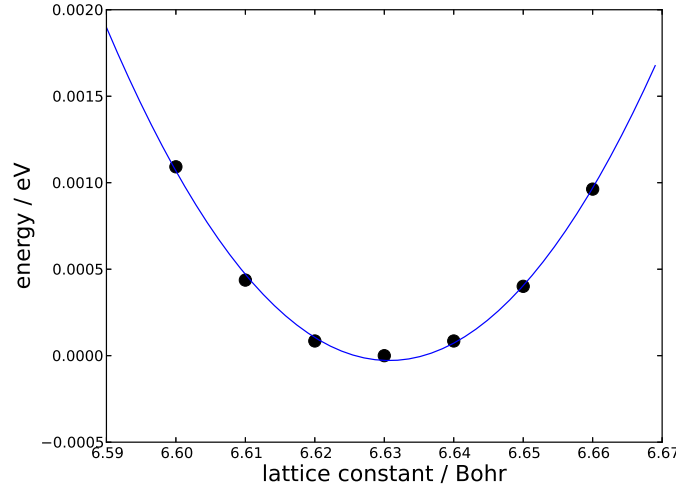


Figure 2. Ground-state energy per particle $E_0(a)/N$ relative to its value at $a = 6.63a_{\text{B}}$ as a function of the fcc lattice parameter a/a_{B} in units of the Bohr radius a_{B} for $(U^{\text{opt}} = 13\text{ eV}, J^{\text{opt}} = 0.9\text{ eV})$, calculated with the full local Hamiltonian $\hat{V}_{\text{loc}}^{\text{full}}$ and the double counting correction $\hat{V}_{\text{dc};1}$. Full line: second-order polynomial fit.

For nickel, detailed information about the quasi-particle bands is available. The quasi-particle dispersion at various high-symmetry points in the Brillouin zone is more sensitive to the precise values of U and J . As we shall show below in more detail, we obtain a satisfactory agreement with ARPES data for the choice $(U^{\text{opt}} = 13\text{ eV}, J^{\text{opt}} = 0.9\text{ eV})$ with an uncertainty of ± 1 in the last digit. For our optimal values we show in Fig. 2 the ground-state energy per particle $E(a)/N$ as a function of the fcc lattice constant a together with a second-order polynomial fit. The minimum is obtained

at $a_0 = 6.63a_B$, in good agreement with the experimental value $a_0^{\text{exp}} = 6.66a_B$. For the magnetic spin-only moment we obtain $m_{\text{so}} = 0.52\mu_B$, in good agreement with the experimental value $m_{\text{so}}^{\text{exp}} = 0.55\mu_B$.

From the curvature of $E(a)/N$ at $a = a_0$ we can extract the bulk modulus. The bulk modulus at zero temperature is defined as the second-derivative of the ground-state energy with respect to the volume,

$$K = V_0 \left. \frac{d^2 E(V)}{dV^2} \right|_{V=V_0}. \quad (109)$$

This implies the Taylor expansion $E(V) = E(V_0) + (KV_0/2)(V/V_0 - 1)^2 + \dots$ for the ground-state energy as a function of the volume $V = a^3$. For the ground-state energy per particle we can thus write $E(a)/N = E(a_0)/N + e_2(a/a_B - a_0/a_B)^2 + \dots$ with

$$e_2 = \frac{9}{8} K a_B^3 (a_0/a_B), \quad (110)$$

where we took into account that the fcc unit cell hosts four atoms, $V_0 = Na_0^3/4$. The fit leads to $K = 169 \text{ GPa}$, in good agreement with the experimental value, $K = 182 \text{ GPa}$ [32]. It is a well-known fact that the DFT-LDA overestimates the bulk modulus of nickel. Indeed, our DFT-LDA gives $K^{\text{LDA}} = 245 \text{ GPa}$.

We also calculated the lattice parameter and the magnetic spin-only moment for the density-dependent interaction $V_{\text{loc}}^{\text{dens}}$, see eq. (98), with the same double-counting correction $\hat{V}_{\text{dc};1}$. Our results do not show significant discrepancies for the ground-state properties. Note, however, that nickel is a special case because it has an almost filled $3d$ -shell ($n_{3d} \approx 9/10$) such that the terms from $\hat{V}_{\text{loc}}^{\text{n.dens.}}$ in eq. (101) are more or less deactivated. Preliminary calculations for iron indicate that the missing interaction terms are more important for a partially filled $3d$ -shell.

The combination of the full local interaction $V_{\text{loc}}^{\text{full}}$ with the second and third double-counting correction, see eqs. (105) and (106), does not lead to reasonable values for the lattice constant, spin-only magnetic moment, and compressibility for nickel. If we fix the lattice constant to its experimental value, the Gutzwiller–Kohn–Sham equations lead to converged results for the second (but not for the third) double-counting correction; for the third double-counting correction, the $3d$ levels are discharged. In the next section, we use these converged results for $\hat{V}_{\text{dc};2}$ for comparison with those for the standard double-counting correction $\hat{V}_{\text{dc};1}$.

5.3.2. Quasi-particle bands of nickel. In Fig. 3 we show the quasi-particle band structure of fcc nickel for ($U^{\text{opt}} = 13 \text{ eV}$, $J^{\text{opt}} = 0.9 \text{ eV}$). The most prominent effect of the Gutzwiller correlator is the reduction of the $3d$ bandwidth. From a paramagnetic DFT-LDA calculation one can deduce $W^{\text{LDA}} = 4.5 \text{ eV}$ [12, 13, 14], whereas we find $W = 3.3 \text{ eV}$, in agreement with experiment. This bandwidth reduction is due to the q -factors $q_{t,\uparrow} = 0.851$, $q_{t,\downarrow} = 0.824$, $q_{e,\uparrow} = 0.852$, $q_{e,\downarrow} = 0.819$, $\bar{q} = \sum_{\sigma} (3q_{t,\sigma} + 2q_{e,\sigma})/10 = 0.837$, so that $W \approx \bar{q}^2 W^{\text{LDA}}$.

A more detailed comparison of the quasi-particle band structure with experiment is given in table 1. The overall agreement between experiment and theory for $\hat{V}_{\text{loc}}^{\text{full}}$ with

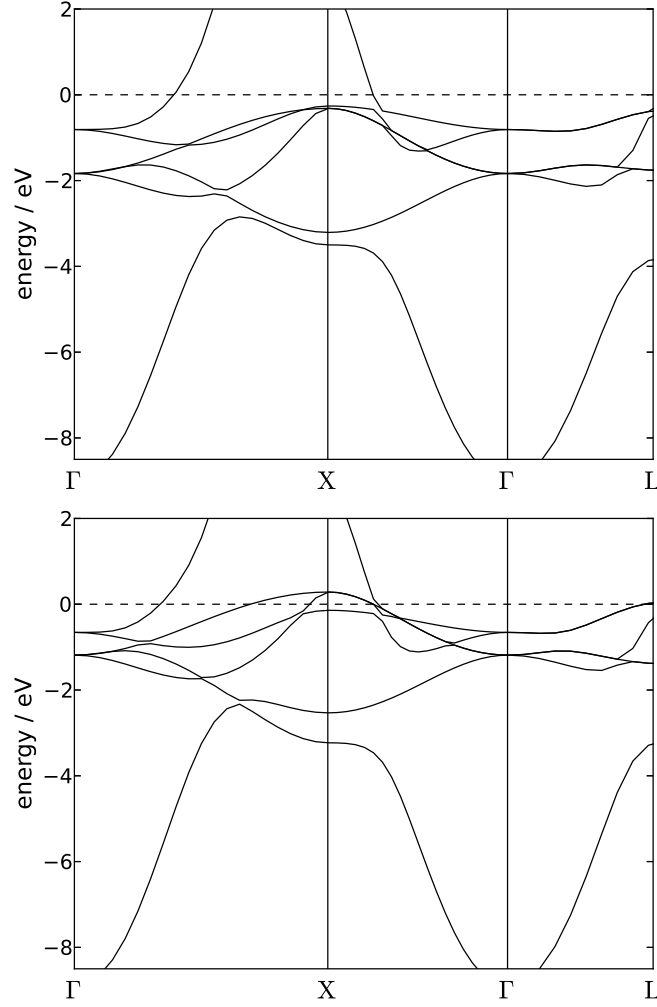


Figure 3. Quasi-particle band structure of fcc nickel along high-symmetry lines in the first Brillouin zone, calculated for $\hat{V}_{\text{loc}}^{\text{full}}$ and $\hat{V}_{\text{dc};1}$ at ($U^{\text{opt}} = 13$ eV, $J^{\text{opt}} = 0.9$ eV). Top: majority spin; Bottom: minority spin. The Fermi energy is at $E_{\text{F}}^{\text{G}} = 0$.

$\hat{V}_{\text{dc};1}$ is quite satisfactory. In particular, only one hole ellipsoid is found at the X -point, in agreement with experiment and in contrast to the DFT-LDA result [8]. Note, however, that the second double-counting correction $\hat{V}_{\text{dc};2}$ spoils this advantage. Therefore, this form of the double-correction term is not particularly useful for nickel.

We comment on two noticeable discrepancies between theory and experiment. First, the energy of the band $L_{2'}$ at the L -point deviates by a factor of five. This is an artifact that occurs already at the DFT-LDA level and is not cured by the Gutzwiller approach. Since the level has pure $3p$ character around the L point, the origin of the discrepancy is related to the uncertainties in the partial charge densities n_{3d} , $n_{3p,3s}$ in the $3d$ and $3p/3s$ bands. Second, the Gutzwiller DFT prediction for the exchange splitting $\Delta_{t_{2g}}(X_5)$ of the t_{2g} bands at the X -point is a factor of two larger than in experiment. This deviation is related to the fact that, quite generally, all bands are slightly too low in energy. This can be cured by decreasing U and increasing J but this deteriorates the values

Symmetry	Experiment	$\hat{V}_{\text{loc}}^{\text{full}}$ & $\hat{V}_{\text{dc};1}$	$\hat{V}_{\text{loc}}^{\text{full}}$ & $\hat{V}_{\text{dc};2}$	$\hat{V}_{\text{loc}}^{\text{dens}}$ & $\hat{V}_{\text{dc};1}$
$\langle \Gamma_1 \rangle$	8.90 ± 0.30	8.95[0.08]	8.99[0.08]	8.93[0.08]
$\langle \Gamma_{25'} \rangle$	1.30 ± 0.06	1.51[0.65]	1.52[0.57]	1.56[0.80]
$\langle \Gamma_{12} \rangle$	0.48 ± 0.08	0.73[0.15]	0.66[0.43]	0.71[0.10]
$\langle X_1 \rangle$	3.30 ± 0.20	3.37[0.27]	3.26[0.56]	3.42[0.10]
$\langle X_3 \rangle$	2.63 ± 0.10	2.87[0.68]	2.87[0.61]	2.87[0.77]
$X_{2\uparrow}$	0.21 ± 0.03	0.26	0.33	0.13
$X_{2\downarrow}$	0.04 ± 0.03	0.14	-0.06	0.21
$X_{5\uparrow}$	0.15 ± 0.03	0.32	0.29	0.41
$\Delta_{e_g}(X_2)$	0.17 ± 0.05	0.12	0.39	-0.08
$\Delta_{t_{2g}}(X_5)$	0.33 ± 0.04	0.60	0.51	0.70
$\langle L_1 \rangle$	3.66 ± 0.10	3.49[0.61]	3.49[0.56]	3.55[0.83]
$\langle L_3 \rangle$	1.43 ± 0.07	1.58[0.38]	1.52[0.52]	1.61[0.26]
$L_{3\uparrow}$	0.18 ± 0.03	0.37	0.38	0.34
$\langle L_{2'} \rangle$	1.00 ± 0.20	0.14[0.06]	0.17[0.06]	0.12[0.06]
$\langle \Lambda_{3;1/2} \rangle$	$0.50[0.21 \pm 0.02]$	0.64[0.30]	0.61[0.45]	0.60[0.16]

Table 1. Quasi-particle band energies with respect to the Fermi energy in eV at various high-symmetry points (counted positive for occupied states). $\langle \dots \rangle$ indicates the spin average, errors bars in the experiments without spin resolution are given as \pm . Theoretical data show the spin average and the exchange splittings in square brackets. $\Lambda_{3;1/2}$ denotes the point half-way on the Λ -line that links the points Γ and L . The first column gives experimental data compiled in [8], the second, third, and fourth column give theoretical results for $\hat{V}_{\text{loc}}^{\text{full}}$ with $\hat{V}_{\text{dc};1}$, $\hat{V}_{\text{loc}}^{\text{full}}$ with $\hat{V}_{\text{dc};2}$, and $\hat{V}_{\text{loc}}^{\text{dens}}$ with $\hat{V}_{\text{dc};1}$, respectively, at ($U^{\text{opt}} = 13 \text{ eV}$, $J^{\text{opt}} = 0.9 \text{ eV}$).

for the lattice constant and the magnetic moment. We suspect that the deviations are partly due to the use of a heuristic double-counting correction and the neglect of the spin-orbit coupling. Moreover, we expect the results for the band structure to improve when we replace the ‘poor-man Wannier’ orbitals for the correlated $3d$ electrons by more sophisticated wave functions.

Table 1 also shows the results for $V_{\text{loc}}^{\text{dens}}$ with density-density interactions only and with $\hat{V}_{\text{dc};1}$ as double-counting correction. The description provides the correct Fermi surface topology but the deviations from the experimental band energies is significantly larger. In particular, the exchange splitting $\Delta_{e_g}(X_2)$ of the e_g bands at the X -point becomes negative, i.e., the order of the majority and minority bands is inverted. The comparison of the band structures shows that the full atomic Hamiltonian should be used for a detailed description of the quasi-particle bands in nickel.

6. Summary and conclusions

In this work, we presented a detailed derivation of the Gutzwiller Density Functional Theory. Unlike previous studies, our formalism covers all conceivable cases of symmetries and Gutzwiller wave functions. Moreover, our theory is not based on the ‘Gutzwiller approximation’ which corresponds to an evaluation of expectation values in the limit of infinite lattice coordination number. It is only in the last step that we resort to this limit.

In particular, our derivation consists of three main steps.

1. The density functional of the full many-particle system is related to that of a reference system with Hubbard-type local Coulomb interactions in the correlated orbitals. This generalizes the widely used Kohn-Sham scheme where a single-particle reference system is used.
2. The energy functional of the Hubbard-type reference system is (approximately) evaluated by means of Gutzwiller variational wave functions.
3. Analytical results for the energy functional are derived with the Gutzwiller approximation.

In a first application we studied the electronic properties of ferromagnetic nickel. It turned out that the Gutzwiller DFT resolves the main deficiencies of DFT in describing ground-state properties such as the lattice constant, the magnetic moment, or the bulk modulus of nickel. Note that our approach requires the relatively large value $U \approx 13$ eV for the local Coulomb interaction in order to obtain a good agreement with experiments.

Our results for the quasi-particle band structure are by and large satisfactory. In fact, a perfect agreement with ARPES data would be surprising because we calculate these quantities based on Fermi-liquid assumptions that are strictly valid only in the vicinity of the Fermi surface. Moreover, the quasi-particle energies strongly depend on the orbital occupations that are influenced by the somewhat arbitrary choice of the double-counting corrections. As we have also shown in this work, different forms of the double-counting correction from the literature lead to fairly different results for nickel. We consider this as the main shortcoming of the Gutzwiller DFT in its present form that should be addressed in future studies.

Appendix A. Single-particle systems

Appendix A.1. Single-particle density matrix

With the help of a single-particle basis $|k\rangle$ in which a given single-particle operator \hat{H}_{sp} is diagonal, an eigenstate can be written as

$$|\Phi\rangle = \prod_k \hat{b}_k^\dagger |\text{vac}\rangle, \quad (\text{A.1})$$

where the prime indicates that N single-particle states are occupied in $|\Phi\rangle$. The single-particle density matrix is diagonal in $|\Phi\rangle$,

$$\rho_{k,k'} \equiv \langle \Phi | \hat{b}_k^\dagger \hat{b}_{k'} | \Phi \rangle = \delta_{k,k'} f_k, \quad (\text{A.2})$$

and the entries on the diagonal obey $f_k^2 = f_k$ because we have $f_k = 0, 1$. Therefore, we have shown that

$$\tilde{\rho} \cdot \tilde{\rho} = \tilde{\rho}. \quad (\text{A.3})$$

Since the operators \hat{c}_i^\dagger for any other single-particle basis and the operators \hat{b}_k^\dagger are related via a unitary transformation, eq. (33) holds generally for single-particle density matrices for single-particle product states.

Appendix A.2. Minimization with respect to the single-particle density matrix

We consider a general real function $E(\tilde{\rho})$ of a non-interacting density matrix $\tilde{\rho}$ with the elements

$$\rho_{i,j} = \langle \Phi | \hat{c}_j^\dagger \hat{c}_i | \Phi \rangle. \quad (\text{A.4})$$

The fact that $\tilde{\rho}$ is derived from a single-particle product wave function $|\Phi\rangle$ is equivalent to the matrix equation (33). Hence, the minimum of $E(\tilde{\rho})$ in the ‘space’ of all non-interacting density matrices is determined by the condition

$$\frac{\partial}{\partial \rho_{j,i}} L(\tilde{\rho}) = 0, \quad (\text{A.5})$$

where we introduced the ‘Lagrange functional’

$$L(\tilde{\rho}) \equiv E(\tilde{\rho}) - \sum_{l,m} \Omega_{l,m} \left(\sum_p \rho_{m,p} \rho_{p,l} - \rho_{m,l} \right) \quad (\text{A.6})$$

and the matrix $\tilde{\Omega}$ of Lagrange parameters $\Omega_{l,m}$. Eq. (A.5) leads to the matrix equation

$$\tilde{H} = \tilde{\rho} \cdot \tilde{\Omega} + \tilde{\Omega} \cdot \tilde{\rho} - \tilde{\Omega} \quad (\text{A.7})$$

for the ‘Hamilton matrix’ \tilde{H} with the elements

$$H_{i,j} = \frac{\partial}{\partial \rho_{j,i}} E(\tilde{\rho}). \quad (\text{A.8})$$

Equation (A.7) is satisfied if eq. (A.3) holds and if

$$[\tilde{H}, \tilde{\rho}] = 0. \quad (\text{A.9})$$

Hence, \tilde{H} and $\tilde{\rho}$ must have the same basis of (single-particle) eigenvectors and, consequently, we find an extremum of $E(\tilde{\rho})$ if we choose $|\Phi\rangle$ as an eigenstate of

$$\hat{H}_{\text{sp}} = \sum_{i,j} H_{i,j} \hat{c}_i^\dagger \hat{c}_j. \quad (\text{A.10})$$

Usually, $|\Phi\rangle$ can be chosen as the ground state of \hat{H}_{sp} .

Appendix A.3. Basis sets

Appendix A.3.1. Kohn-Sham Hamiltonian in its eigenbasis. In the following we assume that the potential is lattice periodic,

$$V_{\sigma}^{\text{KS}}(\mathbf{r}) = U(\mathbf{r}) + V_{\text{Har}}(\mathbf{r}) + v_{\text{sp,xc},\sigma}(\mathbf{r}) = V_{\sigma}^{\text{KS}}(\mathbf{r} + \mathbf{R}) , \quad (\text{A.11})$$

where \mathbf{R} is a lattice vector. The Fourier components are finite only for reciprocal lattice vectors \mathbf{G} ,

$$V_{\mathbf{G},\sigma}^{\text{KS}} = \frac{1}{V} \int d\mathbf{r} V_{\sigma}^{\text{KS}}(\mathbf{r}) e^{-i\mathbf{G}\cdot\mathbf{r}} , \quad (\text{A.12})$$

where V is the crystal volume. As a consequence of the lattice periodicity, the crystal momentum \mathbf{k} from the first Brillouin zone is a good quantum number.

As seen from eq. (41), the Kohn-Sham Hamiltonian is diagonalized for the single-particle states $\psi_{\mathbf{k},n,\sigma}(\mathbf{r}) = \langle \mathbf{r} | \mathbf{k}, n, \sigma \rangle$ that obey

$$h_{\sigma}^{\text{KS}}(\mathbf{r}) \psi_{\mathbf{k},n,\sigma}(\mathbf{r}) = \epsilon_{n,\sigma}(\mathbf{k}) \psi_{\mathbf{k},n,\sigma}(\mathbf{r}) , \quad (\text{A.13})$$

where n is the band index. Eqs. (A.13) are the Kohn-Sham equations [1].

In its eigenbasis, the Kohn-Sham Hamiltonian takes the form

$$\hat{H}^{\text{KS}} = \sum_{\mathbf{k},n,\sigma} \epsilon_{n,\sigma}(\mathbf{k}) \hat{b}_{\mathbf{k},n,\sigma}^{\dagger} \hat{b}_{\mathbf{k},n,\sigma} . \quad (\text{A.14})$$

Its ground state is given by

$$|\Phi_0\rangle = \prod_{\sigma} \prod'_{\mathbf{k},n} \hat{b}_{\mathbf{k},n,\sigma}^{\dagger} |\text{vac}\rangle , \quad (\text{A.15})$$

where the N levels lowest in energy are occupied as indicated by the prime at the product, $\epsilon_{n,\sigma}(\mathbf{k}) \leq E_{\text{F},\sigma}$. Then,

$$f_{\mathbf{k},n,\sigma} = \langle \Phi_0 | \hat{b}_{\mathbf{k},n,\sigma}^{\dagger} \hat{b}_{\mathbf{k},n,\sigma} | \Phi_0 \rangle = \Theta(E_{\text{F},\sigma} - \epsilon_{n,\sigma}(\mathbf{k})) \quad (\text{A.16})$$

is unity for occupied levels up to the Fermi energy $E_{\text{F},\sigma}$, and zero otherwise.

From eq. (26), the field operators read

$$\hat{\Psi}_{\sigma}(\mathbf{r}) = \sum_{\mathbf{k},n} \psi_{\mathbf{k},n,\sigma}(\mathbf{r}) \hat{b}_{\mathbf{k},n,\sigma} , \quad \hat{\Psi}_{\sigma}^{\dagger}(\mathbf{r}) = \sum_{\mathbf{k},n} \psi_{\mathbf{k},n,\sigma}^{*}(\mathbf{r}) \hat{b}_{\mathbf{k},n,\sigma}^{\dagger} . \quad (\text{A.17})$$

Therefore, the ground-state density is readily obtained as

$$\begin{aligned} n_{\sigma}^0(\mathbf{r}) &= \langle \Phi_0 | \hat{\Psi}_{\sigma}^{\dagger}(\mathbf{r}) \hat{\Psi}_{\sigma}(\mathbf{r}) | \Phi_0 \rangle = \sum_{\mathbf{k},n} f_{\mathbf{k},n,\sigma} |\psi_{\mathbf{k},n,\sigma}(\mathbf{r})|^2 = \langle \mathbf{r} | \sum_{\mathbf{k}} \hat{\rho}_{\sigma}^{(0)}(\mathbf{k}) | \mathbf{r} \rangle , \\ \hat{\rho}_{\sigma}^{(0)}(\mathbf{k}) &= \sum_n f_{\mathbf{k},n,\sigma} |\mathbf{k}, n, \sigma\rangle \langle \mathbf{k}, n, \sigma| , \end{aligned} \quad (\text{A.18})$$

see also eq. (31). Since this quantity enters the Kohn-Sham Hamiltonian, its solution must be achieved self-consistently.

Appendix A.3.2. Plane wave basis. In many codes, the Kohn-Sham Hamiltonian is formulated in the plane-wave basis $|\mathbf{k}, \mathbf{G}, \sigma\rangle$ with real-space representation

$$\langle \mathbf{r} | \mathbf{k}, \mathbf{G}, \sigma \rangle = \sqrt{\frac{1}{V}} e^{i(\mathbf{k}+\mathbf{G})\cdot\mathbf{r}} . \quad (\text{A.19})$$

In this basis, the field operators are given by

$$\hat{\Psi}_\sigma(\mathbf{r}) = \sqrt{\frac{1}{V}} \sum_{\mathbf{k}, \mathbf{G}} e^{-i(\mathbf{k}+\mathbf{G})\cdot\mathbf{r}} \hat{p}_{\mathbf{k}, \mathbf{G}, \sigma} , \quad \hat{\Psi}_\sigma^\dagger(\mathbf{r}) = \sqrt{\frac{1}{V}} \sum_{\mathbf{k}, \mathbf{G}} e^{i(\mathbf{k}+\mathbf{G})\cdot\mathbf{r}} \hat{p}_{\mathbf{k}, \mathbf{G}, \sigma}^\dagger , \quad (\text{A.20})$$

and the Kohn-Sham Hamiltonian reads

$$\hat{H}^{\text{KS}} = \sum_{\mathbf{k}, \sigma} \sum_{\mathbf{G}, \mathbf{G}'} T_{\mathbf{G}, \mathbf{G}'; \sigma}^{\text{KS}}(\mathbf{k}) \hat{p}_{\mathbf{k}, \mathbf{G}, \sigma}^\dagger \hat{p}_{\mathbf{k}, \mathbf{G}', \sigma} . \quad (\text{A.21})$$

Eq. (29) shows that the entries of the Kohn-Sham Hamiltonian in reciprocal space are given by

$$T_{\mathbf{G}, \mathbf{G}'; \sigma}^{\text{KS}}(\mathbf{k}) = \delta_{\mathbf{G}, \mathbf{G}'} \frac{1}{2m} (\mathbf{k} + \mathbf{G})^2 + V_{\mathbf{G}-\mathbf{G}'; \sigma}^{\text{KS}} \quad (\text{A.22})$$

for each \mathbf{k} from the first Brillouin zone. The eigenvalues of the Kohn-Sham matrix in reciprocal space are $\epsilon_{\mathbf{n}, \sigma}(\mathbf{k})$, and the solution of the eigenvalue equation [1]

$$\frac{1}{2m} (\mathbf{k} + \mathbf{G})^2 C_{\mathbf{G}, \mathbf{n}, \sigma}(\mathbf{k}) + \sum_{\mathbf{G}'} V_{\mathbf{G}-\mathbf{G}'; \sigma}^{\text{KS}} C_{\mathbf{G}', \mathbf{n}, \sigma}(\mathbf{k}) = \epsilon_{\mathbf{n}, \sigma}(\mathbf{k}) C_{\mathbf{G}, \mathbf{n}, \sigma}(\mathbf{k}) \quad (\text{A.23})$$

for given (\mathbf{k}, \mathbf{n}) gives the entries of the eigenvectors, $C_{\mathbf{G}, \mathbf{n}, \sigma}(\mathbf{k}) = \langle \mathbf{k}, \mathbf{G}, \sigma | \mathbf{k}, \mathbf{n}, \sigma \rangle$. Implemented plane-wave codes provide the band energies $\epsilon_{\mathbf{n}, \sigma}(\mathbf{k})$ and the coefficients $C_{\mathbf{G}, \mathbf{n}, \sigma}(\mathbf{k})$ so that the Kohn-Sham eigenstates are obtained as

$$|\mathbf{k}, \mathbf{n}, \sigma\rangle = \sum_{\mathbf{G}} C_{\mathbf{G}, \mathbf{n}, \sigma}(\mathbf{k}) |\mathbf{k}, \mathbf{G}, \sigma\rangle ,$$

$$\psi_{\mathbf{k}, \mathbf{n}, \sigma}(\mathbf{r}) = \sqrt{\frac{1}{V}} \sum_{\mathbf{G}} C_{\mathbf{G}, \mathbf{n}, \sigma}(\mathbf{k}) e^{i(\mathbf{k}+\mathbf{G})\cdot\mathbf{r}} . \quad (\text{A.24})$$

Appendix A.3.3. Orbital Wannier and Bloch basis. In order to make contact with many-particle approaches based on Hubbard-type models, we need to identify orbitals that enter the local two-particle interaction. Implemented plane-wave codes provide the transformation coefficients $F_{(\mathbf{k}, \mathbf{n}), (\mathbf{R}, b); \sigma}$ from Bloch eigenstates $|\mathbf{k}, \mathbf{n}, \sigma\rangle$ to orbital Wannier states $|\mathbf{R}, b, \sigma\rangle$,

$$|\mathbf{R}, b, \sigma\rangle = \sum_{\mathbf{k}, \mathbf{n}} F_{(\mathbf{k}, \mathbf{n}), (\mathbf{R}, b); \sigma} |\mathbf{k}, \mathbf{n}, \sigma\rangle , \quad F_{(\mathbf{k}, \mathbf{n}), (\mathbf{R}, b); \sigma} = \langle \mathbf{k}, \mathbf{n}, \sigma | \mathbf{R}, b, \sigma \rangle . \quad (\text{A.25})$$

The Wannier orbitals

$$\phi_{\mathbf{R}, b, \sigma}(\mathbf{r}) = \langle \mathbf{r} | \mathbf{R}, b, \sigma \rangle \quad (\text{A.26})$$

are maximal around a lattice site \mathbf{R} and the orbital index b resembles atomic quantum numbers, e.g., $b = 3s, 3p, 3d$. In the orbital Wannier basis the field operators are given by

$$\hat{\Psi}_\sigma^\dagger(\mathbf{r}) = \sum_{\mathbf{R}, b} \phi_{\mathbf{R}, b, \sigma}^*(\mathbf{r}) \hat{c}_{\mathbf{R}, b, \sigma}^\dagger , \quad \hat{\Psi}_\sigma(\mathbf{r}) = \sum_{\mathbf{R}, b} \phi_{\mathbf{R}, b, \sigma}(\mathbf{r}) \hat{c}_{\mathbf{R}, b, \sigma} , \quad (\text{A.27})$$

and the Kohn-Sham Hamiltonian in the orbital Wannier basis becomes

$$\hat{H}^{\text{KS}} = \sum_{\mathbf{R}, b, \mathbf{R}', b', \sigma} T_{(\mathbf{R}, b), (\mathbf{R}', b'); \sigma}^{\text{KS}} \hat{c}_{\mathbf{R}, b, \sigma}^\dagger \hat{c}_{\mathbf{R}', b', \sigma} \quad (\text{A.28})$$

with the overlap matrix elements

$$T_{(\mathbf{R}, b), (\mathbf{R}', b'); \sigma}^{\text{KS}} = \int d\mathbf{r} \phi_{\mathbf{R}, b, \sigma}^*(\mathbf{r}) h_\sigma^{\text{KS}}(\mathbf{r}) \phi_{\mathbf{R}', b', \sigma}(\mathbf{r}) , \quad (\text{A.29})$$

see eq. (41). These matrix elements appear in a tight-binding representation of the kinetic energy in Hubbard-type models.

For later use we also define the orbital Bloch basis,

$$\phi_{\mathbf{k}, b, \sigma}(\mathbf{r}) = \sqrt{\frac{1}{L}} \sum_{\mathbf{R}} e^{i\mathbf{k} \cdot \mathbf{R}} \phi_{\mathbf{R}, b, \sigma}(\mathbf{r}) , \quad \phi_{\mathbf{R}, b, \sigma}(\mathbf{r}) = \sqrt{\frac{1}{L}} \sum_{\mathbf{k}} e^{-i\mathbf{k} \cdot \mathbf{R}} \phi_{\mathbf{k}, b, \sigma}(\mathbf{r}) , \quad (\text{A.30})$$

where \mathbf{k} is from the first Brillouin zone and L is the number of lattice sites. The field operators are given by

$$\hat{\Psi}_\sigma^\dagger(\mathbf{r}) = \sum_{\mathbf{k}, b} \phi_{\mathbf{k}, b, \sigma}^*(\mathbf{r}) \hat{c}_{\mathbf{k}, b, \sigma}^\dagger , \quad \hat{\Psi}_\sigma(\mathbf{r}) = \sum_{\mathbf{k}, b} \phi_{\mathbf{k}, b, \sigma}(\mathbf{r}) \hat{c}_{\mathbf{k}, b, \sigma} . \quad (\text{A.31})$$

In the orbital Wannier basis, the Kohn-Sham single-particle Hamiltonian reads

$$\begin{aligned} \hat{H}^{\text{KS}} &= \sum_{\mathbf{k}, b, b', \sigma} T_{b, b'; \sigma}^{\text{KS}}(\mathbf{k}) \hat{c}_{\mathbf{k}, b, \sigma}^\dagger \hat{c}_{\mathbf{k}, b', \sigma} , \\ T_{b, b'; \sigma}^{\text{KS}}(\mathbf{k}) &= \int d\mathbf{r} \phi_{\mathbf{k}, b, \sigma}^*(\mathbf{r}) h_\sigma^{\text{KS}}(\mathbf{r}) \phi_{\mathbf{k}, b', \sigma}(\mathbf{r}) . \end{aligned} \quad (\text{A.32})$$

Appendix B. Plane-wave basis for the Gutzwiller quasi-particle Hamiltonian

Appendix B.1. Gutzwiller quasi-particle Hamiltonian in first quantization.

The Gutzwiller quasi-particle Hamiltonian in eq. (79) defines a single-particle problem in second quantization. In order to express it in first quantization, we define the single-particle operators

$$\begin{aligned} \hat{\eta}_\sigma(\mathbf{k}) &= \sum_{b, b'} \eta_{b, b'; \sigma} |\mathbf{k}, b, \sigma\rangle \langle \mathbf{k}, b', \sigma| , \\ \hat{Q}_\sigma(\mathbf{k}) &= \sum_{a, b} q_{a, \sigma}^{b, \sigma} |\mathbf{k}, b, \sigma\rangle \langle \mathbf{k}, a, \sigma| . \end{aligned} \quad (\text{B.1})$$

The operator $\hat{\eta}_\sigma(\mathbf{k})$ is Hermitian.

As seen from eqs. (79) and (84), in the orbital Bloch basis we have

$$\hat{H}_{\text{qp}}^{\text{G}} = \sum_{\mathbf{k}, b, b', \sigma} \langle \mathbf{k}, b, \sigma | \left[\hat{Q}_\sigma(\mathbf{k}) \hat{h}_{0, \sigma}(\mathbf{k}) \hat{Q}_\sigma^\dagger(\mathbf{k}) + \hat{\eta}_\sigma(\mathbf{k}) \right] | \mathbf{k}, b', \sigma \rangle \hat{c}_{\mathbf{k}, b, \sigma}^\dagger \hat{c}_{\mathbf{k}, b', \sigma} , \quad (\text{B.2})$$

where

$$\begin{aligned} \hat{h}_{0, \sigma}(\mathbf{k}) &= \sum_{b, b'} h_{b, b'; \sigma}^0(\mathbf{k}) |\mathbf{k}, b, \sigma\rangle \langle \mathbf{k}, b', \sigma| \\ &= \sum_{\mathbf{G}, \mathbf{G}'} h_{\mathbf{G}, \mathbf{G}'; \sigma}^0(\mathbf{k}) |\mathbf{k}, \mathbf{G}, \sigma\rangle \langle \mathbf{k}, \mathbf{G}', \sigma| . \end{aligned} \quad (\text{B.3})$$

Note that for the non-interacting limit, $\lambda_{\Gamma,\Gamma'} = 1$, we have $q_{a,\sigma}^{b,\sigma} = \delta_{a,b}$, $\hat{Q}_\sigma(\mathbf{k}) = \hat{1}$, and $\hat{\eta}_\sigma(\mathbf{k}) = 0$ so that $\hat{H}_{\text{qp}}^{\text{G}}$ reduces to \hat{H}^{KS} in eq. (A.32). Eq. (B.2) shows that the Gutzwiller quasi-particle Hamiltonian in first quantization reads

$$\hat{h}_{\text{qp}}^{\text{G}} = \sum_{\mathbf{k},\sigma} \left[\hat{Q}_\sigma(\mathbf{k}) \hat{h}_\sigma^0(\mathbf{k}) \hat{Q}_\sigma^\dagger(\mathbf{k}) + \hat{\eta}_\sigma(\mathbf{k}) \right]. \quad (\text{B.4})$$

This comparison proves relations used in previous studies [9, 10, 11].

In the orbital Bloch basis we define the operator for the single-particle density matrix in first quantization as

$$\hat{\rho}_\sigma^{\text{G}}(\mathbf{k}) = \sum_{b,b'} \rho_{b,b';\sigma}^{\text{G}}(\mathbf{k}) |\mathbf{k}, b, \sigma\rangle \langle \mathbf{k}, b', \sigma|, \quad (\text{B.5})$$

with $\rho_{b,b';\sigma}^{\text{G}}(\mathbf{k})$ from eq. (83) where

$$\rho_{b,b';\sigma}(\mathbf{k}) = \langle \Phi_0 | \hat{c}_{\mathbf{k},b',\sigma}^\dagger \hat{c}_{\mathbf{k},b,\sigma} | \Phi_0 \rangle = \langle \mathbf{k}, b, \sigma | \hat{\rho}_\sigma(\mathbf{k}) | \mathbf{k}, b', \sigma \rangle \quad (\text{B.6})$$

are the matrix elements for the optimized single-particle product state $|\Phi_0\rangle$. We define the projection operator $\hat{\rho}_\sigma(\mathbf{k})$ onto the occupied Gutzwiller quasi-particle states

$$\hat{\rho}_\sigma(\mathbf{k}) = \sum_n f_{\mathbf{k},n,\sigma}^{\text{G}} |\mathbf{k}, n, \sigma\rangle^{\text{G}} \langle \mathbf{k}, n, \sigma|, \quad (\text{B.7})$$

see eq. (89). With these definitions, we can readily express the local densities in eq. (61)

$$n_\sigma(\mathbf{r}) = \langle \mathbf{r} | \sum_{\mathbf{k}} \hat{\rho}_\sigma^{\text{G}}(\mathbf{k}) | \mathbf{r} \rangle. \quad (\text{B.8})$$

Using the further assumption that the local single-particle density matrix \tilde{C} is diagonal and that $q_{a,\sigma}^{b,\sigma} = \delta_{a,b} q_{a,\sigma}$, we recover the expressions for the single-particle density matrix used in previous investigations [9, 10].

Appendix B.2. Quasi-particle Hamiltonian in the plane-wave basis.

Using the notation of Appendix B.1, we can readily express the Gutzwiller quasi-particle operator in the plane-wave basis,

$$\hat{h}_{\text{qp}}^{\text{G}} = \sum_{\mathbf{k}, \mathbf{G}, \mathbf{G}', \sigma} \langle \mathbf{k}, \mathbf{G}, \sigma | \left[\hat{Q}_\sigma(\mathbf{k}) \hat{h}_\sigma^0(\mathbf{k}) \hat{Q}_\sigma^\dagger(\mathbf{k}) + \hat{\eta}_\sigma(\mathbf{k}) \right] | \mathbf{k}, \mathbf{G}', \sigma \rangle \hat{p}_{\mathbf{k}, \mathbf{G}, \sigma}^\dagger \hat{p}_{\mathbf{k}, \mathbf{G}', \sigma}. \quad (\text{B.9})$$

This representation shows that we have to diagonalize the Gutzwiller–Kohn–Sham plane-wave matrix with the entries

$$h_{\mathbf{G}, \mathbf{G}'; \sigma}^{\text{G}}(\mathbf{k}) = \sum_{\mathbf{G}_1, \mathbf{G}_2} \left[Q_{\mathbf{G}, \mathbf{G}_1; \sigma}(\mathbf{k}) h_{\mathbf{G}_1, \mathbf{G}_2; \sigma}^0(\mathbf{k}) Q_{\mathbf{G}', \mathbf{G}_2; \sigma}^*(\mathbf{k}) \right] + \hat{\eta}_{\mathbf{G}, \mathbf{G}'; \sigma}(\mathbf{k}), \quad (\text{B.10})$$

where

$$\begin{aligned} Q_{\mathbf{G}, \mathbf{G}'; \sigma}(\mathbf{k}) &= \sum_{a,b} q_{a,\sigma}^{b,\sigma} \langle \mathbf{k}, \mathbf{G}, \sigma | \mathbf{k}, b, \sigma \rangle \langle \mathbf{k}, a, \sigma | \mathbf{k}, \mathbf{G}', \sigma \rangle, \\ h_{\mathbf{G}, \mathbf{G}'; \sigma}^0(\mathbf{k}) &= \delta_{\mathbf{G}, \mathbf{G}'} \frac{1}{2m} (\mathbf{k} + \mathbf{G})^2 + V_{\mathbf{G}-\mathbf{G}', \sigma}^{\text{H}}, \\ \eta_{\mathbf{G}, \mathbf{G}'; \sigma}(\mathbf{k}) &= \sum_{b,b'} \eta_{b,b'; \sigma} \langle \mathbf{k}, \mathbf{G}, \sigma | \mathbf{k}, b, \sigma \rangle \langle \mathbf{k}, b', \sigma | \mathbf{k}, \mathbf{G}', \sigma \rangle, \end{aligned} \quad (\text{B.11})$$

for each \mathbf{k} from the first Brillouin zone. The eigenvalues of the Gutzwiller matrix are $\epsilon_{\mathbf{n},\sigma}^G(\mathbf{k})$, and the entries of the eigenvectors are $C_{\mathbf{G},\mathbf{n},\sigma}^G(\mathbf{k})$ so that

$$|\mathbf{k}, \mathbf{n}, \sigma\rangle^G = \sum_{\mathbf{G}} C_{\mathbf{G},\mathbf{n},\sigma}^G(\mathbf{k}) |\mathbf{k}, \mathbf{G}, \sigma\rangle \quad (\text{B.12})$$

defines the Gutzwiller quasi-particle eigenstates in the plane-wave basis. From those states we can derive ‘correlated orbital Bloch states’ $|\mathbf{k}, c, \sigma\rangle^G$ that can be used to define the operators in eq. (B.1) self-consistently. The correlations induce shape-changes of the Wannier orbitals, i.e., $\phi_{\mathbf{R},c,\sigma}^G(\mathbf{r}) = \langle \mathbf{r} | \mathbf{R}, c, \sigma \rangle^G$ deviates from the original Wannier orbital $\phi_{\mathbf{R},c,\sigma}(\mathbf{r})$. Therefore, the correlated orbitals can be determined self-consistently. We find that the effect is negligibly small for nickel.

Appendix C. Atomic Hamiltonian in cubic symmetry

We choose the Hubbard parameters $U(u, v), U(\zeta, \zeta), U(\xi, \eta), U(\zeta, u), U(\zeta, v)$, the four Hund’s-rule couplings $J(u, v), J(\xi, \eta), J(\zeta, u), J(\zeta, v)$, and the two-particle transfer matrix element $S(\eta, \xi; \zeta, u)$ as our ten independent Coulomb matrix elements in cubic symmetry. The other matrix elements in eq. (101) can be expressed as [25]

$$\begin{aligned} U(u, u) &= U(v, v) = U(u, v) + 2J(u, v) , \\ U(\xi, u) &= U(\eta, u) = (U(\zeta, u) + 3U(\zeta, v))/4 , \\ U(\xi, v) &= U(\eta, v) = (3U(\zeta, u) + U(\zeta, v))/4 , \\ J(\xi, u) &= J(\eta, u) = (J(\zeta, u) + 3J(\zeta, v))/4 , \\ J(\xi, v) &= J(\eta, v) = (3J(\zeta, u) + J(\zeta, v))/4 , \\ \\ T(\eta; u, v) &= -T(\xi; u, v) = \sqrt{3}(U(\zeta, u) - U(\zeta, v))/4 , \\ A(\eta; u, v) &= -A(\xi; u, v) = \sqrt{3}(J(\zeta, u) - J(\zeta, v))/4 , \\ \\ S(\xi, \eta; \zeta, u) &= S(\eta, \xi; \zeta, u) , \\ S(\zeta, \xi; \eta, u) &= -2S(\eta, \xi; \zeta, u) , \\ S(\xi, \eta; \zeta, v) &= -\sqrt{3}S(\eta, \xi; \zeta, u) , \\ S(\zeta, \xi; \eta, u) &= \sqrt{3}S(\eta, \xi; \zeta, u) . \end{aligned} \quad (\text{C.1})$$

If we further assume that the radial part of the t_{2g} -orbitals and the e_g -orbitals are identical (‘spherical approximation’), we may express all matrix elements in terms of three parameters, e.g., the Racah parameters A, B , and C that are related to the Slater-Condon parameters by $A = F^{(0)} - F^{(4)}/9$, $B = (F^{(2)} - 5F^{(4)}/9)/49$, and $C = 5F^{(4)}/63$. In particular,

$$\begin{aligned} U(u, v) &= A - 4B + C , \\ J(u, v) &= 4B + C , \\ U(\zeta, \zeta) &= A + 4B + 3C , \\ U(\xi, \eta) &= A - 2B + C , \\ J(\xi, \eta) &= 3B + C , \\ U(\zeta, u) &= A - 4B + C , \end{aligned}$$

$$\begin{aligned}
U(\zeta, v) &= A + 4B + C , \\
J(\zeta, v) &= C , \\
J(\zeta, u) &= 4B + C , \\
S(\eta, \xi; \zeta, u) &= -\sqrt{3}B .
\end{aligned} \tag{C.2}$$

The average Coulomb interaction between electrons in same orbitals is given by

$$U = \frac{1}{5} \sum_{c=\xi, \eta, \zeta, u, v} U(c, c) = A + 4B + 3C , \tag{C.3}$$

the average Coulomb interaction between electrons in different orbitals is given by

$$U' = \frac{1}{10} \sum_{c, c'=\xi, \eta, \zeta, u, v; c < c'} U(c, c') = A - B + C , \tag{C.4}$$

and the average Hund's-rule coupling becomes

$$J = \frac{1}{10} \sum_{c, c'=\xi, \eta, \zeta, u, v; c < c'} J(c, c') = \frac{5}{2}B + C . \tag{C.5}$$

- [1] For an overview, see Martin R M, *Electronic Structure* (Cambridge University Press, Cambridge, 2004); Dreizler R M and Gross E K U, *Density Functional Theory* (Springer, Berlin, 1990).
- [2] Moruzzi V L, Janak J F and Williams A R, *Calculated Electronic Properties of Metals* (Pergamon Press, New York, 1978).
- [3] Hubbard J, Proc. Roy. Soc. A **276**, 238 (1963).
- [4] Gutzwiller M C, Phys. Rev. Lett. **10**, 159 (1963).
- [5] Anisimov V I, Aryasetiawan F and Lichtenstein A I, J. Phys.: Condens. Matter **9**, 767 (1997).
- [6] Kotliar G, Savrasov S, Haule K, Oudovenko V, Parcollet O and Marianetti C, Rev. Mod. Phys. **78**, 865 (2006).
- [7] Pavarini E, Koch E, Vollhardt D and Lichtenstein A (editors), *The LDA+DMFT approach to strongly correlated materials* (Schriften des Forschungszentrums Jülich, Reihe Modelling and Simulation, vol. 1, 2011).
- [8] Bünnemann J, Gebhard F and Weber W, in *Frontiers in Magnetic Materials*, edited by A. Narlikar (Springer, Berlin, 2005), p. 117; arXiv:cond-mat/0503332.
- [9] Ho K M, Schmalian J and Wang C Z, Phys. Rev. B **77**, 073101 (2008); Yao Y X, Schmalian J, Wang C Z, Ho K M and Kotliar G, Phys. Rev. B **84**, 245112 (2011); Lanatà N, Yao Y-X, Wang C-Z, Ho K M, Schmalian J, Haule K and Kotliar G, Phys. Rev. Lett. **111**, 196801 (2013).
- [10] Wang G-T, Dai X and Fang Z, Phys. Rev. Lett. **101**, 066403 (2008); Deng X, Dai X and Fang Z, Eur. Phys. Lett. **83**, 37008 (2008); Deng X, Wang L, Dai X and Fang Z, Phys. Rev. B **79**, 075114 (2009); Wang G-T, Qian Y, Xu G, Dai X and Fang Z, Phys. Rev. Lett. **104**, 047002 (2010); Tian M-F, Deng X, Fang Z and Dai X, Phys. Rev. B **84**, 205124 (2011).
- [11] Dong R, Wan X, Dai X and Savrasov S Y, Phys. Rev. B **89**, 165122 (2014).
- [12] Bünnemann J, Gebhard F, Ohm T, Umstätter R, Weiser S, Weber W, Claessen R, Ehm D, Harasawa A, Kakizaki A, Kimura A, Nicolay G, Shin S and Strocov V N, Europhys. Lett. **61**, 667 (2003).
- [13] Bünnemann J, Gebhard F, Ohm T, Weiser S and Weber W, Phys. Rev. Lett. **101**, 236404 (2008).
- [14] Hofmann A, Cui X, Schäfer J, Meyer S, Höpfner P, Blumenstein C, Paul M, Patthey L, Rotenberg E, Bünnemann J, Gebhard F, Ohm T, Weber W and Claessen R, Phys. Rev. Lett. **102**, 187204 (2009).
- [15] Schickling T, Gebhard F, Bünnemann J, Boeri L, Andersen O K and Weber W, Phys. Rev. Lett. **108**, 036406 (2012).
- [16] Lu F, Zhao J, Weng H, Fang Z and Dai X, Phys. Rev. Lett. **110**, 096401 (2013); Weng H, Zhao J, Wang Z, Fang Z and Dai X Phys. Rev. Lett. **112**, 016403 (2014).
- [17] Levy M, Phys. Rev. A **26**, 1200 (1982); Lieb E H, Int. J. Quan. Chem. **24**, 243 (1983).
- [18] The condition (22) is too strong. We can equally work with $\tilde{D}_{\text{sp}}[\{n_{\sigma}(\mathbf{r})\}] = D_{\text{sp}}[\{n_{\sigma}(\mathbf{r})\}] + \Delta[\{n_{\sigma}(\mathbf{r})\}]$ as long as $\Delta[\{n_{\sigma}^0(\mathbf{r})\}] = 0$ and $(\partial\Delta[\{n_{\sigma}(\mathbf{r})\}]/(\partial n_{\sigma}(\mathbf{r}))|_{n_{\sigma}(\mathbf{r})=n_{\sigma}^0(\mathbf{r})} = 0$. Then, $\tilde{D}_{\text{sp}}[\{n_{\sigma}(\mathbf{r})\}]$ leads to the same ground-state energy and ground-state density as $D_{\text{sp}}[\{n_{\sigma}(\mathbf{r})\}]$.
- [19] Bünnemann J in *Correlated Electrons: From Models to Materials*, ed. by Pavarini E, Koch E, Anders F and Jarrell M (Schriften des Forschungszentrums Jülich, Reihe Modelling and Simulation, vol. 2, 2012), chap. 5.
- [20] Gebhard F, Phys. Rev. B **41**, 9452 (1990).
- [21] Bünnemann J, Schickling T and Gebhard F, Europhys. Lett. **98**, 27006 (2012).
- [22] Kaczmarczyk J, Spalek J, Schickling T and Bünnemann J, Phys. Rev. B **88**, 115127 (2013).
- [23] Bünnemann J, Weber W and Gebhard F, Phys. Rev. B **57**, 6896 (1998).
- [24] Bünnemann J, Schickling T, Gebhard F and Weber W, physica status solidi (b) **249**, 1282 (2012).
- [25] Sugano S, Tanabe Y and Kamimura H, *Multiplets of Transition-Metal Ions in Crystals* (Pure and Applied Physics **33**, Academic Press, New York, 1970).
- [26] Blöchl P E, Pruschke T and Potthoff M, Phys. Rev. B **88**, 205139 (2013).
- [27] Giannozzi P, Baroni S, Bonini N, Calandra M, Car R, Cavazzoni C, Ceresoli D, Chiarotti G L, Cococcioni M, Dabo I, Dal Corso A, Fabris S, Fratesi G, de Gironcoli S, Gebauer R, Gerstmann U, Gougoussis C, Kokalj A, Lazzeri A, Martin-Samos L, Marzari N, Mauri F, Mazzarello R, Paolini S, Pasquarello A, Paulatto L, Sbraccia C, Scandolo S, Sclauzero G, Seitsonen A P,

- Smogunov A, Umari P, Wentzcovitch R M, J. Phys.: Condens. Matter **21**, 395502 (2009);
<http://www.quantum-espresso.org/>
- [28] Bünenmann J, Gebhard F and Thul R, Phys. Rev. B **67**, 075103 (2003).
- [29] Schnell I, Czycholl G and Albers R C, Phys. Rev. B **65**, 075103 (2002).
- [30] Aryasetiawan F, Imada M, Georges A, Kotliar G, Biermann S and Lichtenstein A I, Phys. Rev. B **70**, 195104 (2004).
- [31] Lichtenstein A I, Katsnelson M I and Kotliar G, Phys. Rev. Lett. **87**, 067205 (2001); Biermann S, Aryasetiawan F and Georges A, Phys. Rev. Lett. **90**, 086402 (2003).
- [32] Zhao D-J, Albe K and Hahn H, Scripta Materialia **55**, 473 (2006).